Western Australian Centre for Geodesy
Curtin University of Technology

Computation of a new gravimetric quasigeoid model for New Zealand

Technical Report

Sten Claessens, Christian Hirt, Will Featherstone, Jonathan Kirby
11/08/2009

Table of Contents

Executive Summary

This report describes the computation of NZGeoid09, a new gravimetric quasigeoid model for New Zealand, computed at the Western Australian Centre for Geodesy under contract #CON-SE-DSS-TS-45245-3 to Land Information New Zealand (LINZ). NZGeoid09 has a spatial resolution of 1′x1′ and spans an area from 160˚E to 190˚E and from 25˚S to 60˚S. It is based on an iterative computation approach that accounts for offsets among New Zealand's 13 different local vertical datums (LVDs).

NZGeoid09 contains several improvements over the previous model NZGeoid05. Firstly, it uses the latest global input data. The EGM2008 global gravity model is used up to degree and order 2160 as a reference model. Marine gravity anomalies from the DNSC08 global model were used in combination with terrain-corrected land gravity anomalies in a Stokesian integration with a deterministically modified kernel. Secondly, the processing strategy was improved. Most notably, the interpolation of land gravity anomalies in coastal areas is augmented through use of DNSC08, area means of reconstituted gravity anomalies are computed using a sophisticated regridding technique, and area means of gravity anomalies from EGM2008 are computed ellipsoidally.

The optimal Stokes integration parameters of degree of modification L = 40 and cap radius ψ_0 = 2.5˚ were determined through a comparison with 1422 GPS/levelling observations. The accuracy of the final NZGeoid09 is assessed using the same GPS/levelling dataset, yielding an overall standard deviation of 6.2 cm after removal of the vertical offsets from the residuals for each LVD. NZGeoid09 performs better than NZGeoid05 and marginally better than the EGM2008 model, but few data are available in the Southern Alps to give a better evaluation.

1 Introduction

This purpose of this report is to describe and document the computation of the new gravimetric quasigeoid model for New Zealand (herein referred to as NZGeoid09) performed at the Western Australian Centre for Geodesy under contract #CON-SE-DSS-TS-45245-3 to Land Information New Zealand (LINZ).

NZGeoid09 is based on the iterative gravimetric quasigeoid computation approach (Amos 2007, Amos and Featherstone 2009) that accounts for offsets among the 13 different local vertical datums (LVDs) in New Zealand. The computation area spans from 160˚E to 190˚E and from 25˚S to 60˚S. NZGeoid09 has a spatial resolution of 1´x1´, as opposed to 2´x2´ for the previous New Zealand quasigeoid model (NZGeoid05). This means that short-wavelength portions of New Zealand's gravity field are better modelled, and interpolation errors for users of the model are reduced.

The most important datasets for the NZGeoid09 computation are a set of 40,737 land (and some littoral zone) gravity observations (Fig. 1), the altimetry-based DNSC08 marine gravity anomaly model, and the EGM2008 global gravity model. DNSC08 and EGM2008 are significant improvements over earlier models used in the computation of NZGeoid05 (cf. Claessens and Anjasmara 2008). As well as the improved resolution and input data quality, several modifications to the data processing scheme used for NZGeoid05 have been made.

Section 2 gives a detailed technical description of the NZGeoid09 computation scheme. The datasets used for NZGeoid09 are described in Section 2.1. The gravity data preparation, the use of the EGM2008 and DNSC08 datasets as well as the Stokes integration and geoid testing using GPS/levelling stations are dealt with in Section 2.2. Finally, the results of the NZGeoid09 computation (with focus on the iterative results and the optimisation of the Stokes integration parameters) are analysed in Section 3. The Appendices contain details on the scripts and directory structures used. A complete visualisation of all data processing steps for a selected test area can be found in Appendix A3.

Note that the following conventions are used in this report: the input datasets are referred to by numbers (1 – 7) and the processing steps are denoted by letters (A – M).

2 Computation of NZGeoid09

2.1 Input datasets

The data sources described below form the basis for the NZGeoid09 quasigeoid model. The numbering of the datasets is in agreement with the numbers used in the flowchart of the NZGeoid09 computation (Fig. 2). All datasets were provided by LINZ, with the exception of sets 3 and 6.

1. *Land gravity anomalies*. On the land and littoral-zone areas (North Island, South Island, Stewart Island and the Chatham Islands), a total of 40,737 gravity observations (Fig. 1) are available at an estimated accuracy level of 0.1-0.5 mGal (Amos 2007).
2. *Terrain correction data.* For the North and South Island, there are 62 tiles (1′ x 1′) available that contain gravimetric terrain corrections computed by brute-force prism integration (Amos 2007, p. 94). The terrain corrections are used for the conversion of (simple) Bouguer anomalies to refined Bouguer anomalies, as well as approximations of the Molodensky terms in quasigeoid computation (cf. Sideris 1990).
3. *DNSC08*. Over marine areas, the altimetry-based DNSC08 free-air anomaly grid (Andersen et al. 2008) is available at a spatial resolution of 1′. This model is based on a pre-release of EGM2008 and uses retracked multi-mission altimeter data, which generally improves the gravity anomalies in the coastal zone (cf. Hwang et al. 2008).
4. *DNSC08 draped*. A combination of DNSC08 gravity anomalies and ship-track gravity anomalies is available as alternative marine gravity dataset on the ocean. However, this dataset was not used in the computation of NZGeoid09 after an evaluation of its quality (showing stripes correlated with the ship-tracks) and consultation with LINZ (Amos, pers. comm. 2009).
5. *Digital elevation model data* (DEM). For the North and South Islands, a high-resolution (56 m grid spacing) national DEM is available. The elevation data is provided in 62 tiles, each covering an area of 1′ x 1′. The DEM data is used for the transformation of gridded refined Bouguer anomalies to Faye anomalies (reconstitution of the topographic effect; Featherstone and Kirby 2000)
6. *EGM2008*. The EGM2008 global geopotential model (Pavlis et al. 2008) is the state-of-the-art spherical harmonic model of the Earth's global gravity field. It is complete up to spherical harmonic degree and order 2160 (this corresponds to wavelengths of roughly 9 km) and also provides the long- and medium wavelength reference (gravity anomalies and height anomalies) for the NZGeoid09 quasigeoid computation.
7. *GPS/levelling*. Directly observed height anomalies (all be they on the different LVDs) are available at 1422 GPS/levelling stations on the North and South Island of New Zealand (none on the Chatham Islands). This set serves as benchmark for quasigeoid testing (accuracy assessment) and, most importantly, enables the iterative quasigeoid computation with LVD unification.

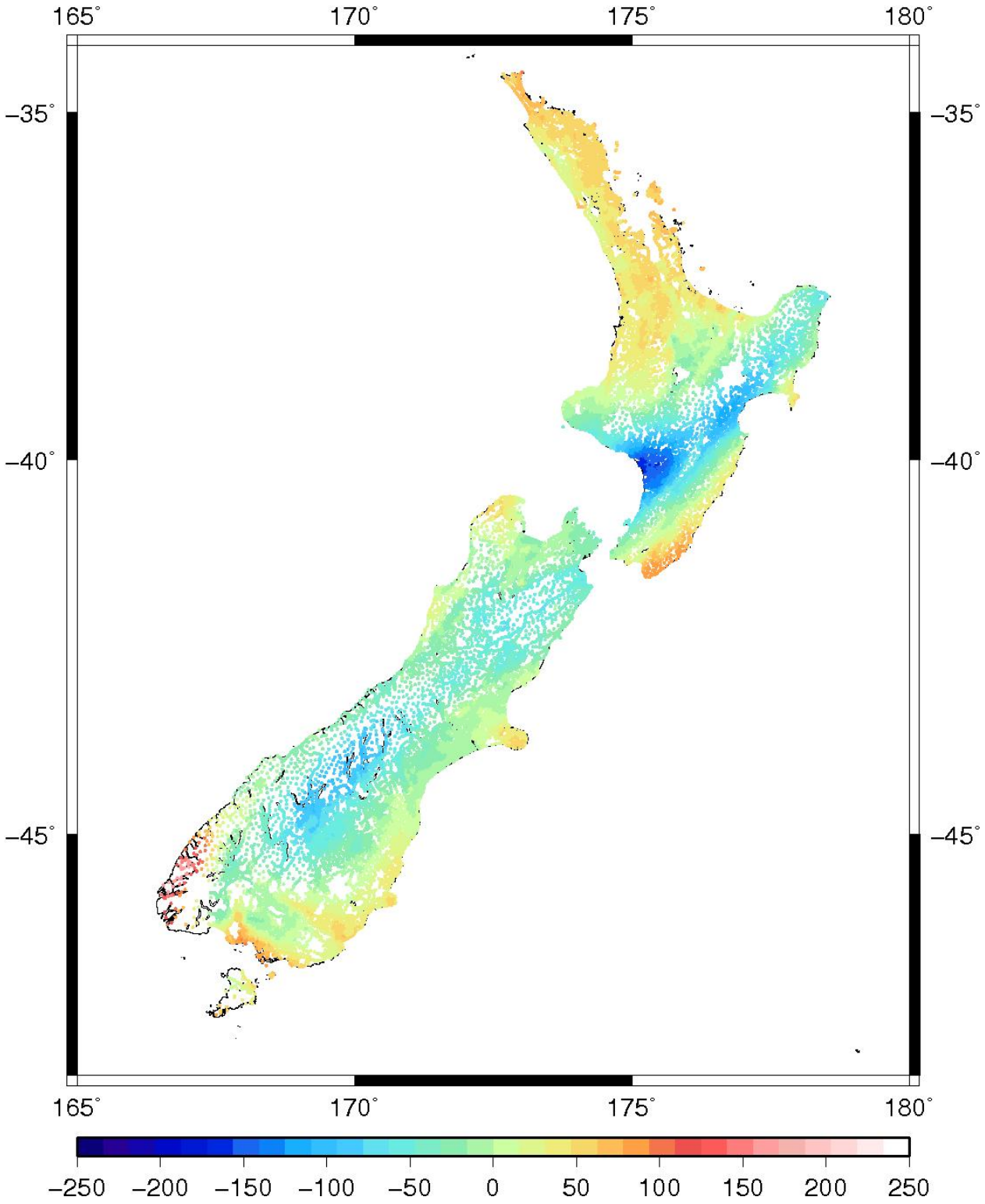

Fig.1. Refined Bouguer anomalies on the North and South Islands of New Zealand
(Mercator projection; units in mGal)

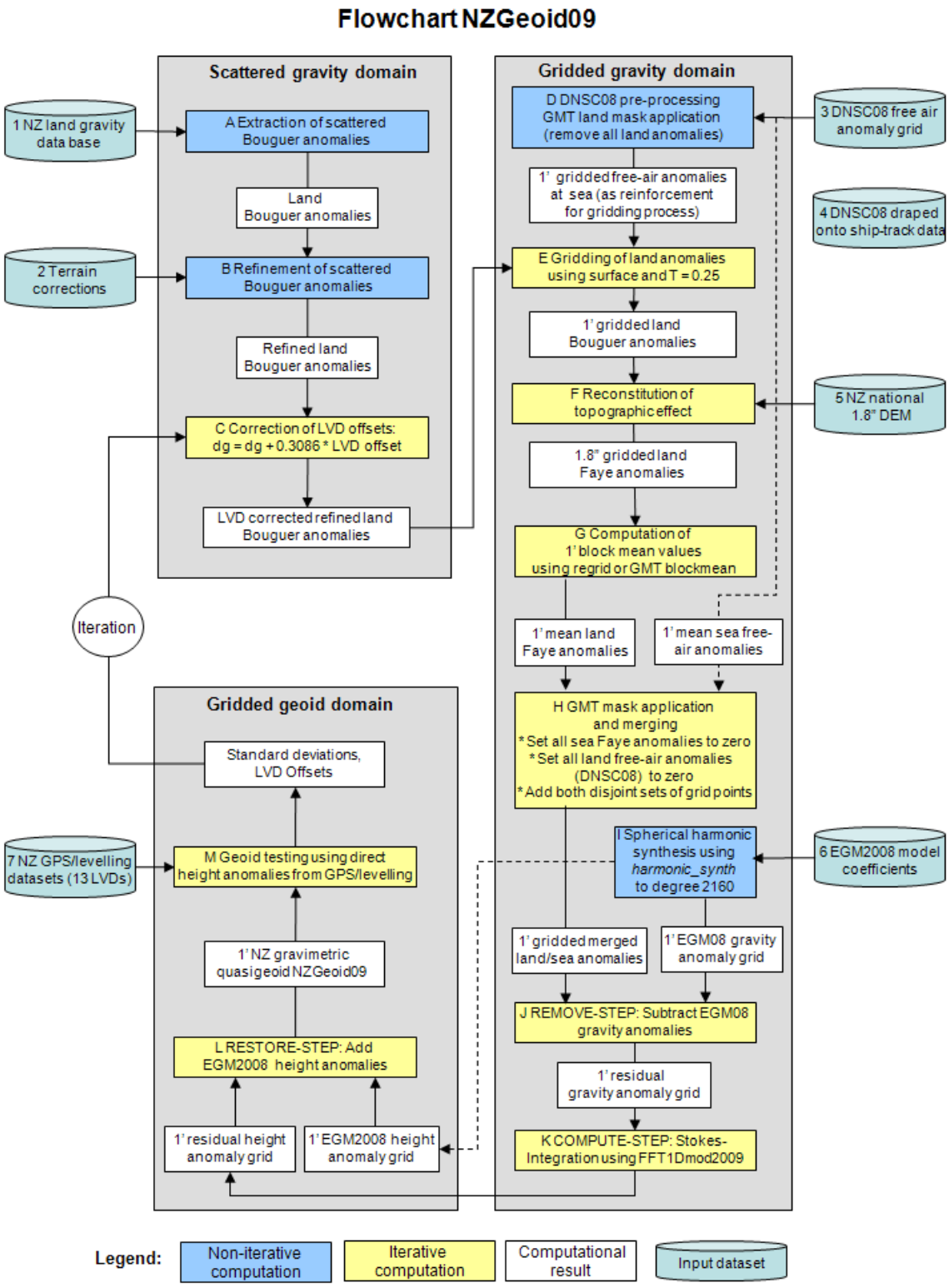

Fig.2. Flowchart for the computation of NZGeoid09

2.2 Detailed description of all processing steps

A general overview of the data processing strategy for NZGeoid09 is provided in Fig. 2. The flowchart shows that 13 main processing steps (blue and yellow boxes, referred to with letters A-M) are required to convert the scattered land gravity observations to a regular 1′x1′ grid of gravimetric quasigeoid heights, and to derive accuracy measures from comparisons with GPS/levelling data (step M).

The seven input datasets, represented by the light blue cylinders in Fig. 2, are shown in the context of the processing steps. Figure 2 shows in detail how the iterative quasigeoid computation scheme (Amos and Featherstone 2009) works: a correction of the gravity data with LVD offsets is applied to the scattered gravity data (step C). The subsequent steps, indicated by yellow boxes in Fig. 2, depend on the LVD offsets and are performed iteratively until the loop converges, i.e., until the LVD offset values (these are the mean values of the residuals between GPS/levelling data and the gravimetric quasigeoid heights) do no longer change significantly. The steps indicated by blue boxes (steps A, B, D, G) are performed just once, i.e., they are only computed in the first iteration and not recomputed in subsequent iterations. Figure 2 also distinguishes between the computation steps dealing with *scattered gravity data*, *gridded gravity data* and with *gridded geoid undulations* by means of grey boxes.

In the following, the processing steps A-M are described in detail. An overview of the improvements to the NZGeoid05 data processing strategy is provided in Section 2.3.

A. and B. Extraction and refinement of Bouguer anomalies

The New Zealand gravity database is provided in terms of simple Bouguer anomalies (e.g., Torge 2001, p. 266), separately for the 13 different LVDs defined by the polygons in Amos and Featherstone (2009). The simple Bouguer anomalies are converted to refined Bouguer anomalies through addition of gravimetric terrain corrections (dataset 2), interpolated bilinearly to the locations of the scattered gravity observations. The terrain corrections account for the difference between a Bouguer plate and the irregular topography (e.g., Forsberg 1984). The left part of Fig. 3 shows the high-resolution DEM for a test tile on the North Island and the right part shows the precomputed terrain corrections. It can be seen that, depending on the variation of topography, terrain corrections typically range from 0 to 10 mGal, with higher values found in mountainous areas.

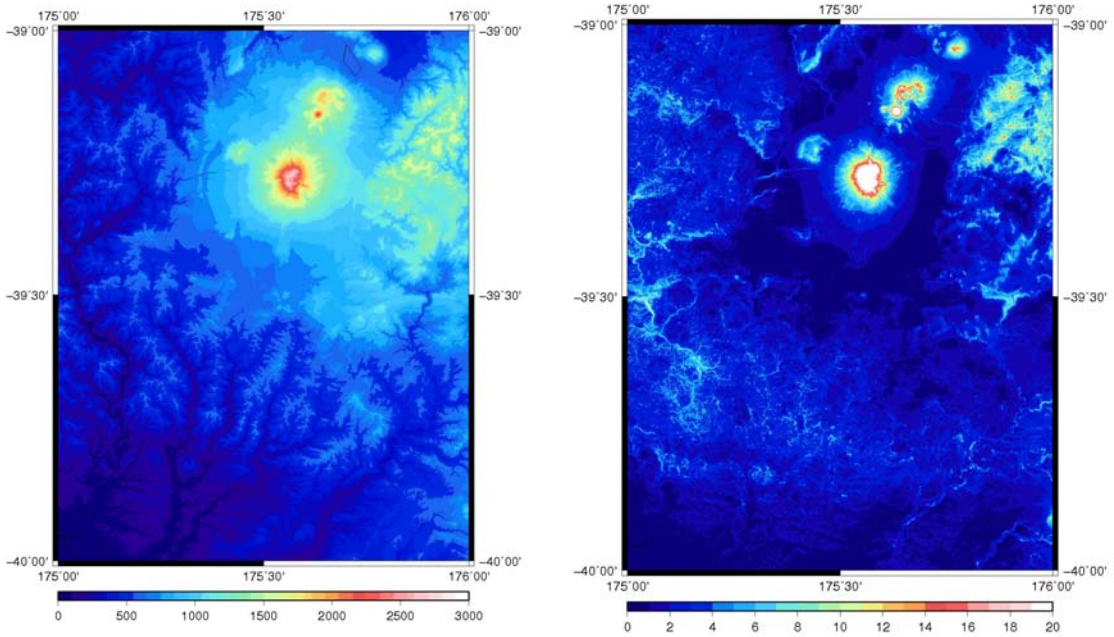

Fig 3. Left: NZ DEM for a test tile (Ruapehu/Whanganui River, North Island) (Mercator projection; units in m); Right: Precomputed grid of terrain corrections (Mercator projection; units in mGal).

C. LVD correction

The LVD correction (or datum offset correction) takes into account that heights of the 13 sets of gravity stations are with respect to different LVDs and thus do not form a consistent dataset. The impact of the datum offset on the refined Bouguer anomalies is computed using the linear approximation of the free-air gravity correction

$$\delta\Delta g = 0.3086 \cdot o \qquad (1)$$

where o is the offset (vertical distance) between the quasigeoid and the LVD (cf. Amos and Featherstone 2009). For each of the 13 LVDs, individual values for o and thus corrections $\delta\Delta g$ are applied to the refined Bouguer anomalies.

Initial values for o were set to 0.00 m for all LVDs. The comparison of the computed quasigeoid (step M) with GPS/levelling stations yields a set of residuals. The mean values of these residuals were used as a measure of the LVD offset o and are reintroduced in an iterative computation (cf. flowchart in Fig. 2).

D. DNSC08 data preparation

The DNSC08 marine gravity model (Anderson et al. 2008) provides a 1′x1′ grid of altimetry-derived free-air anomalies over the oceans. On land, the DNSC08 model uses EGM2008 free-air anomalies as fill-in data. The DNSC08 free-air anomalies were extracted from the DNSC08 database using the standard grid extensions 160°/190° longitude and -60°/-25° latitude (cf. Fig. 4, left). In the context of the NZGeoid09

computation, the DNSC08 free-air anomaly grid accomplishes two tasks. First, it is used as reinforcement for the interpolation of land gravity Bouguer anomalies so they are not incorrectly extrapolated over the littoral zone (step E). Second, it provides the gravity input data for the ocean areas (step H). In both cases, data on land areas are appropriately excluded using the GMT (Generic Mapping Tools; Wessel and Smith 1998) land mask operation along with the full-resolution GMT coastline database (cf. Fig. 4, right).

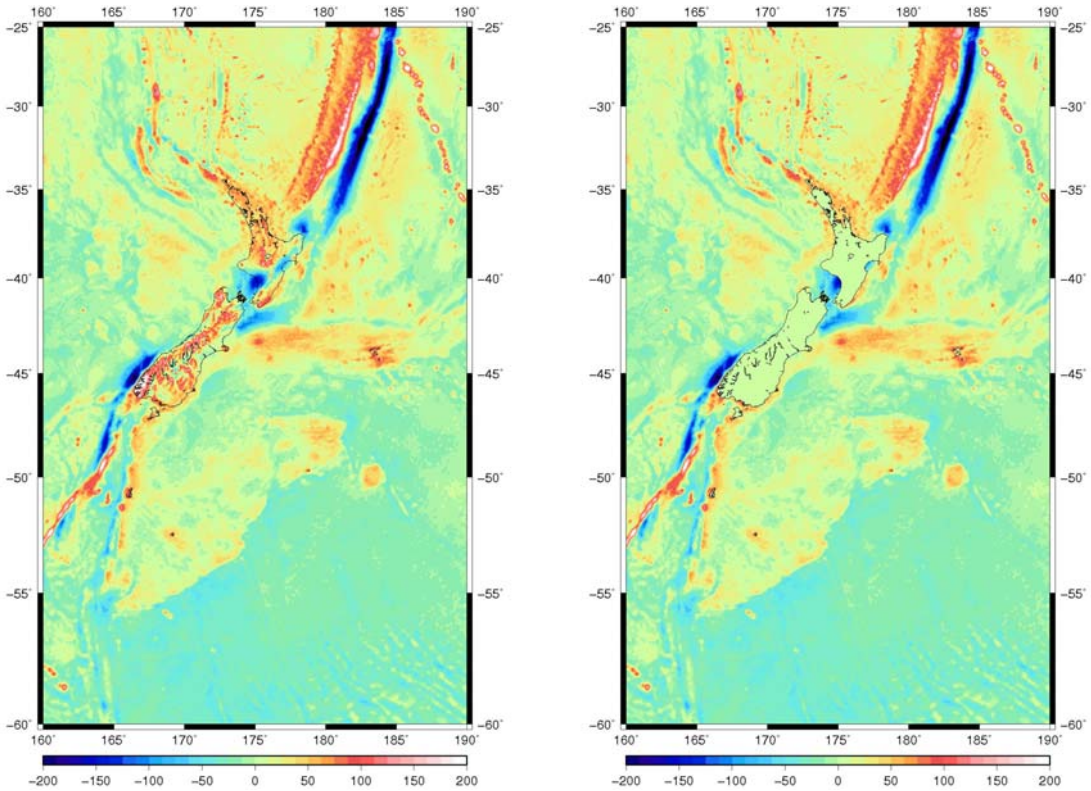

Fig 4. Left: DNSC08 free-air anomalies for the NZGeoid09 computation area; Right: DNSC08 free-air anomalies with the land areas excluded (Mercator projection; units in mGal)

E. Gridding of Bouguer anomalies

The generation of a regular 1′x1′ grid of refined Bouguer anomalies is performed using the GMT *surface* function. The algorithm of this function interpolates the grid points using continuous curvature splines in tension with a user-defined tension factor *T*. For potential fields, the recommended tension factor of $T = 0.25$ was used (Smith and Wessel 1990).

Over the littoral zone and beyond, the gridding of the land Bouguer anomalies (e.g., using *surface*) tends to be unreliable due to the distribution of the gravity stations causing unwanted extrapolation. Therefore, the land Bouguer anomaly dataset was augmented with marine gravity data (DNSC08 free-air anomalies) before interpolation. Figure 5 demonstrates how this approach reinforces the interpolation of land Bouguer anomalies. Figures 5A and 5B show the scattered and interpolated land Bouguer anomalies in the Northwest Nelson region (South Island).

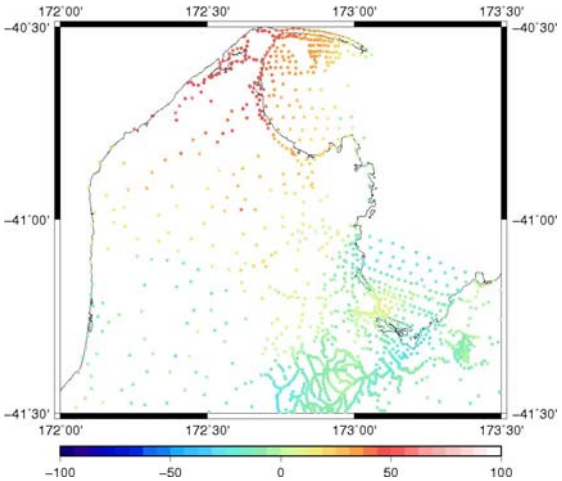

A: Land Bouguer anomalies at scattered locations in the test area, without DNSC08 data

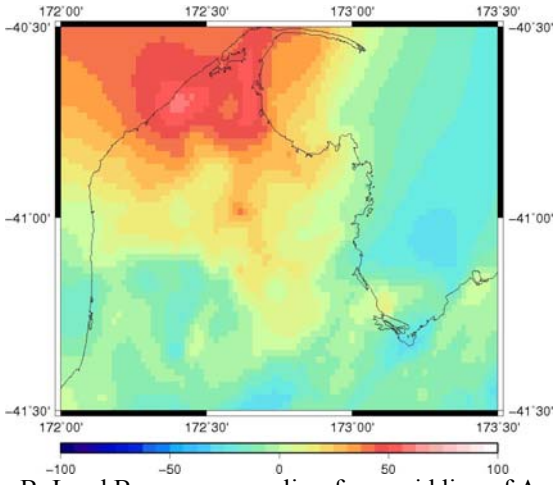

B: Land Bouguer anomalies, from gridding of A using *surface*

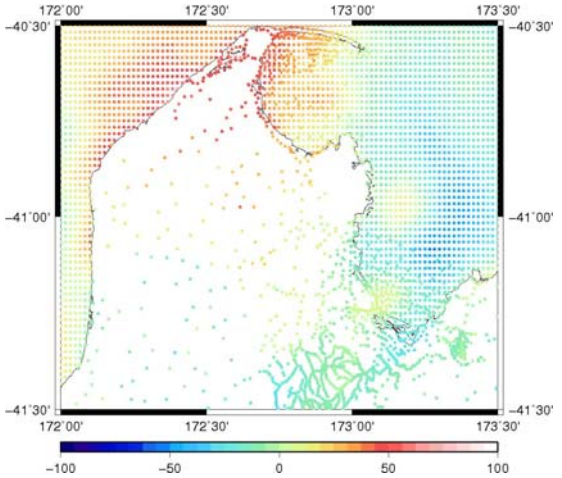

C: Land Bouguer anomalies merged with DNSC08 at scattered locations in the test area.

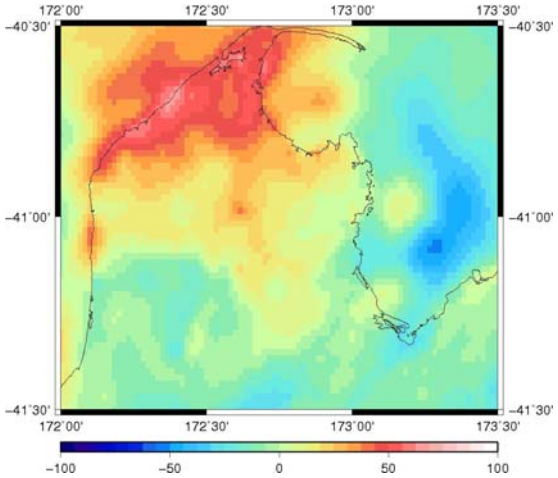

D: Land Bouguer anomalies, from gridding of C using *surface*

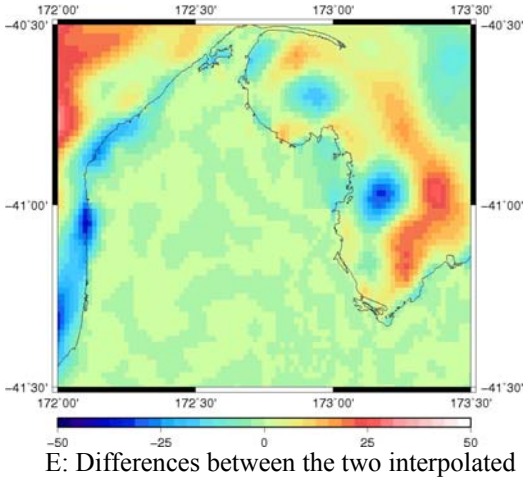

E: Differences between the two interpolated Bouguer anomaly grids

Fig.5. Reinforcement of Bouguer anomaly interpolation in a coastal region (Northwest Nelson, South Island) (Mercator projections; units in mGal)

The land Bouguer anomalies, supplemented with the DNSC08 dataset is depicted in Fig. 5C. Importantly, the DNSC08 dataset was masked over land, so that the fill-in data from EGM2008 were excluded. The interpolated grid based on this merged land/sea dataset is depicted in Fig. 5D. Figure 5E shows the differences between the two interpolated grids (Figs. 5B and 5D), demonstrating that extrapolation errors of the order of 10 mGal are avoided, which would have occurred when interpolating the land only data without DNSC08 augmentation, especially in areas with few land gravity observations near the coast.

F. Reconstitution of the topography

To reduce spatial aliasing and to generate mean gravity anomalies needed for the numerical integrations (step K), mean gravity anomalies were reconstituted from the gridded refined Bouguer land gravity anomalies using the reconstitution technique described in Featherstone and Kirby (2000) and Amos (2007). For this reconstitution step, the high-resolution (national) DEM (resolution 56 m or 1.8″ in NS-direction) was used. The refined Bouguer anomalies were interpolated bilinearly to the centre of each DEM cell, and the topography was reconstituted using the reverse planar Bouguer correction for the DEM height with a constant topographic mass density of 2670 kg.m^{-3}. This procedure gives *terrain-corrected free-air* anomalies, which are also referred to as *Faye* anomalies. However, this terminology is somewhat loose because the terrain corrections approximate the G1 Molodensky term required for quasigeoid computation (cf. Sideris, 1990).

The reconstitution as described above is carried out for all 62 1˚x1˚ DEM tiles. It converts the 1´x1´ Bouguer anomaly grid to a very dense 1.8″x1.8″ Faye (free-air plus Molodensky G1 term) anomaly grid. This is shown for the test area "Ruapehu/Whanganui River" (North Island) in Fig. 6.

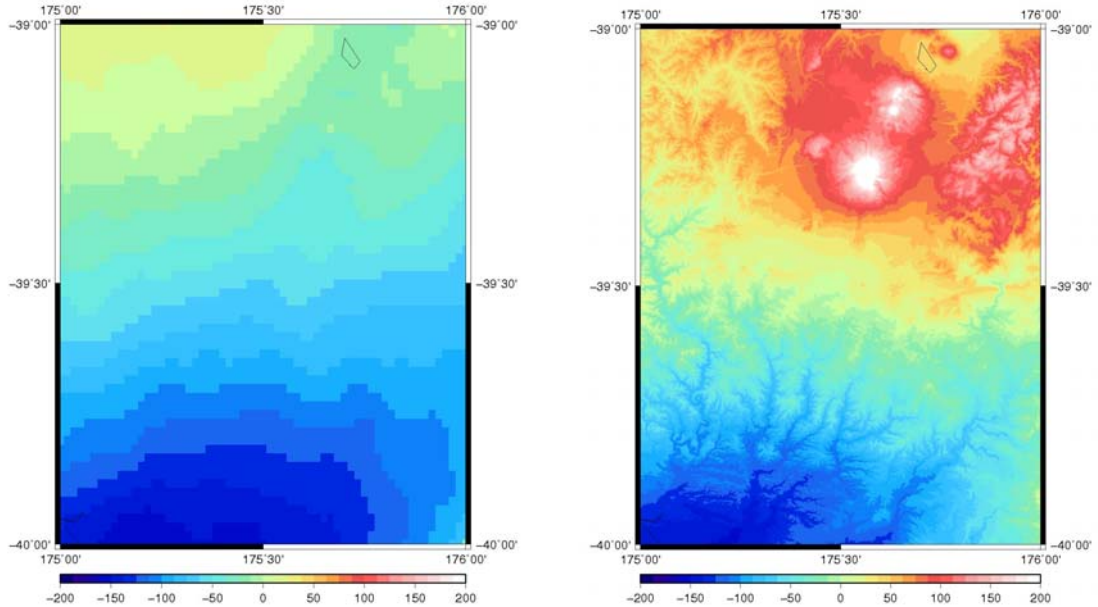

Fig. 6. Left: gridded refined Bouguer anomalies; Right: Faye anomalies, obtained from interpolated refined Bouguer anomalies by reconstitution of the topography (Mercator projections; units in mGal)

The software routines used for the reconstitution (*ni_reconstitute_1min* and *si_reconstitute_1min*) were validated using two test runs, with elevation data and refined Bouguer anomaly data set to zero, respectively, followed by a comparison of the results to the original refined Bouguer anomalies and elevation data (cf. Appendix A3). This verified that the technique and software were operating correctly.

G. Computation of area mean anomalies

The 1.8″x1.8″ Faye anomaly grid was regridded to a coarser 1´x1´ resolution using sophisticated regridding software (*regrid_sid*) developed at the Western Australian Centre for Geodesy. This software was selected over the GMT *blockmean* function, because *blockmean* does not properly account for input grid cells that are only partly inside the output grid cell. The regridding software used here includes these cells into the computation of the area mean, weighted by the area percentage that is inside the output grid cell. Validation with area means computed using spherical harmonic integration formulas has shown that regridding errors using *regrid_sid* are two orders of magnitude smaller than using *blockmean*. In addition, boundary errors resulting from the merger of 1°x1° tiles are negligible (<10µGal) using *regrid_sid*.

The 62 regridded 1°x1° tiles were eventually merged to one data file (Fig. 7).

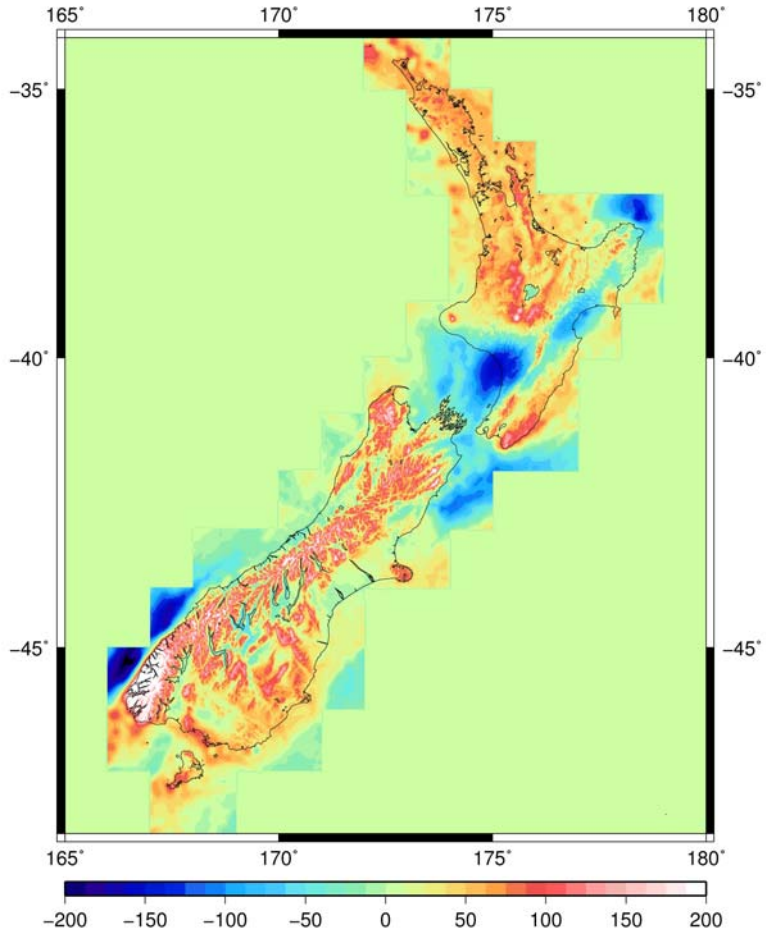

Fig. 7. 62 merged 1°x1° tiles with 1'x1' reconstituted and regridded Faye anomalies over NZ (Mercator projection, units in mGal). Note that the data offshore will not be used in the computations.

H. Merging of land and marine anomalies

Step H comprises the merging of the land Faye anomalies (from step G) and the DNSC08 marine free-air anomalies (from step D). The merging is accomplished using the GMT *grdlandmask* function along with the high-resolution GMT shoreline database. The high-resolution land mask is applied to the Faye anomalies so that all data points on oceanic areas are set to zero (Fig. 8, left) and, analogously, a sea mask applied to the DNSC08 free-air anomalies sets all land points to zero (cf. Fig. 3, right). The resulting two masked grids represent complementary sets of gravity anomalies. They were added together to produce the final 1´x1´ grid of merged land/sea anomalies (Fig. 8, right).

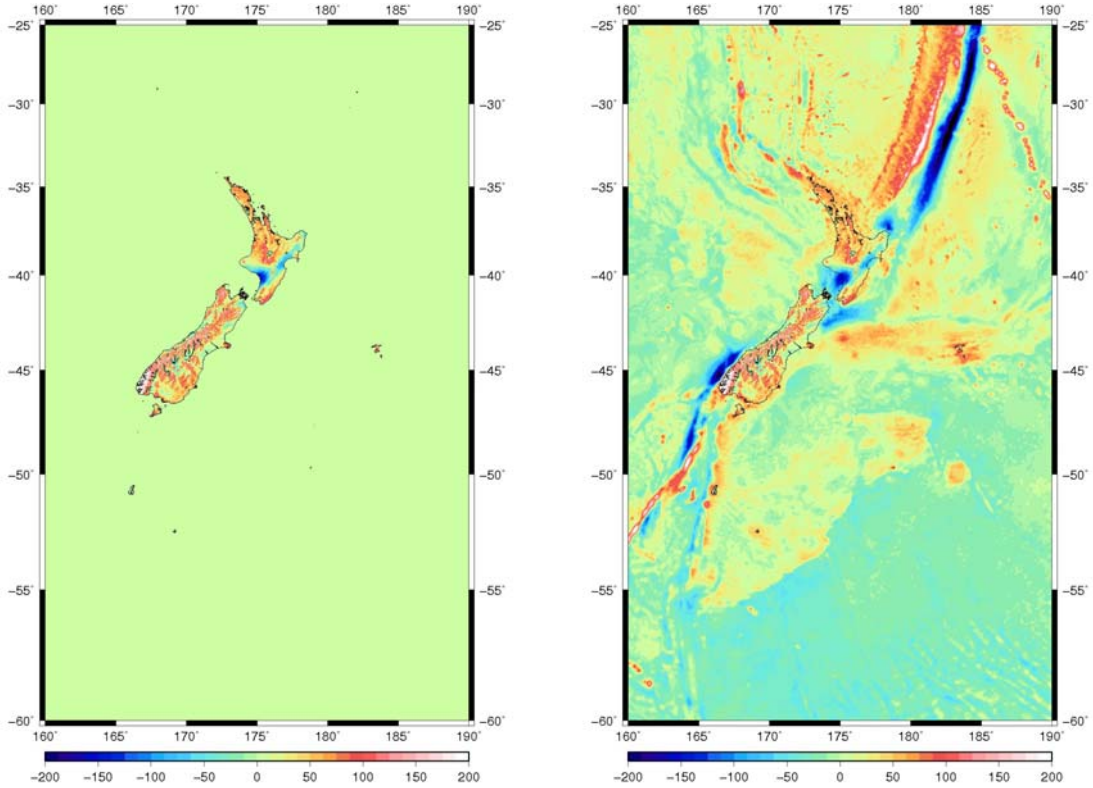

Fig. 8. Left: masked land Faye anomalies; Right: merged land/sea anomalies
(Mercator projections; units in mGal)

I. Spherical harmonic synthesis using EGM2008

The state-of-the-art EGM2008 global gravity model (Pavlis et al., 2008) provides the height anomaly (quasigeoid height) and gravity anomaly reference fields for NZGeoid09 (Fig. 9). The spherical harmonic synthesis of the coefficients of EGM2008 is performed using the *harmonic_synth* software provided by the EGM2008 development team. All data synthesised from EGM2008 were computed in the zero-tide system. The spectral range used is degree and order 2 to 2160, which corresponds to a spatial wavelength of ~9 km. Because of the zero degree term, the resulting quasigeoid computation is subject to a vertical offset with an order of magnitude of several decimetres. See step M for an explanation on the role of the zero degree term on testing with GPS/levelling data.

The gravity anomaly grid computed from EGM2008 consists of 1′x1′ area means of gravity anomalies in ellipsoidal approximation. A spherical approximation is not sufficient in this step, because it could lead to errors in the quasigeoid with a magnitude of several decimetres (Hipkin, 2004, Claessens, 2006). Ellipsoidal area means cannot be computed rigorously, but were computed by adding an ellipsoidal correction to area means of gravity anomalies in spherical approximation. Comparison to area means computed from a dense grid of point values in ellipsoidal approximation over a 2˚x2˚ test tile on the South Island (167˚E-169˚E, 46˚S-44˚S) show that the error in the ellipsoidal correction is negligible (<10 μGal).

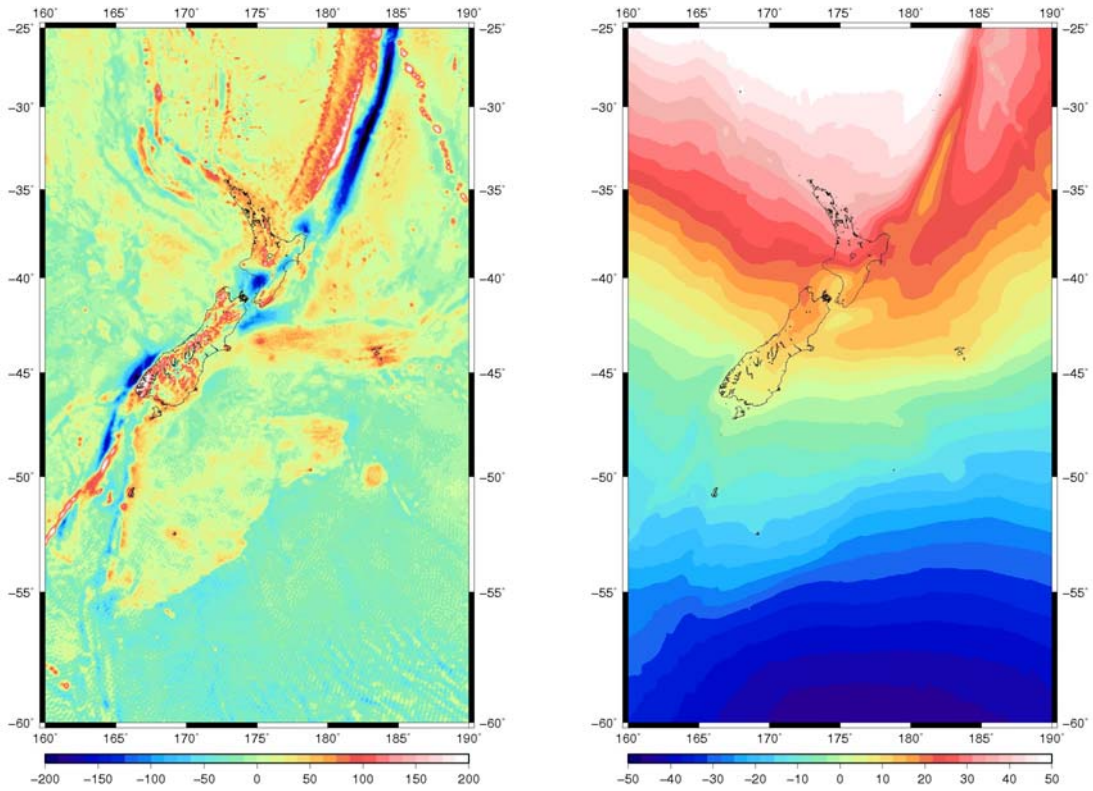

Fig. 9. Left: EGM2008 gravity anomaly grid (area means in ellipsoidal approximation) (Mercator projection; units in mGal); Right: EGM2008 height anomaly grid (Mercator projection; units in m)

J. Removal of the reference field

In order to obtain the residual gravity field, the EGM2008 gravity anomaly field (step I) is algebraically subtracted from the merged land/sea gravity anomalies (step H). Figure 10 shows, for the central part of the NZGeoid09 computation area, that the subtraction of the EGM2008 reference field removes a large part of the gravity field signal. This is also seen from the descriptive statistics of the three gravity grids in Table 1.

Table 1. Descriptive statistics of the NZ land/sea anomalies, EGM2008 gravity anomalies and the residual gravity anomalies (units in mGal)

grid	min	max	mean	std.dev	RMS
Land/sea gravity anomalies	-252.96	311.80	1.98	35.28	35.33
EGM2008 gravity anomalies in ellipsoidal approximation	-250.67	307.18	1.97	35.09	35.15
Residual gravity anomalies	-186.76	143.93	0.01	4.69	4.69

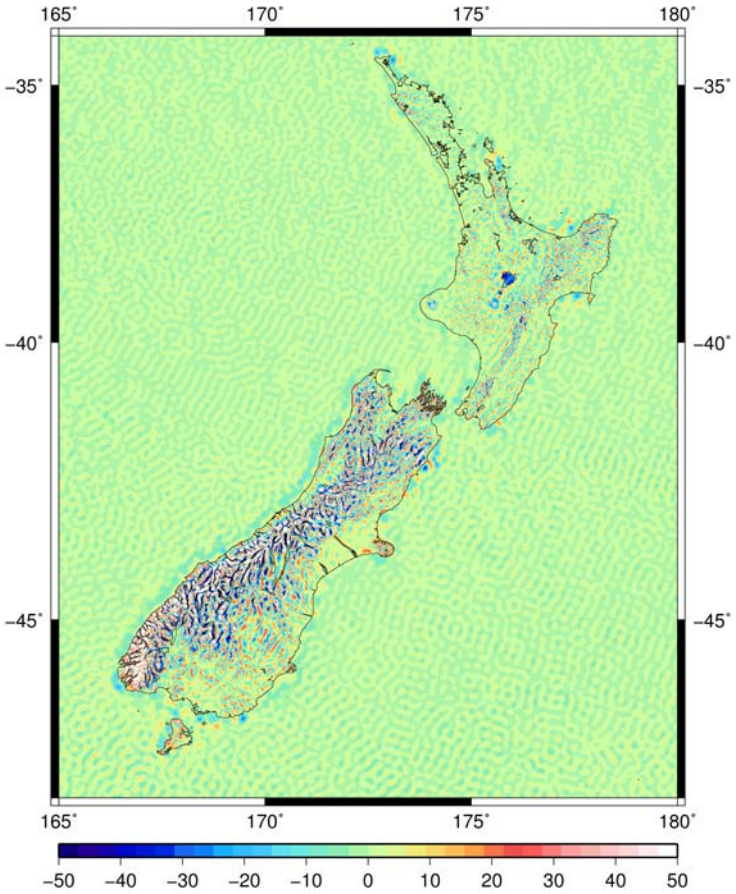

Fig. 10. Residual gravity anomaly grid in the central NZGeoid09 computation area (Mercator projection, units in mGal). The larger residual anomalies on the South Island are due to rugged topography.

K. Stokesian integrations

The transformation of the gridded mean residual gravity anomalies to a grid of point residual quasigeoid heights is performed using *FFT1Dmod2009* developed at the Western Australian Centre for Geodesy. This program performs Stokes integration using a deterministically modified integration kernel (Featherstone et al. 1998), and the 1D-fast Fourier transform (FFT) numerical integration technique by Haagmans et al. (1992). It was upgraded in 2009 to deliver a better estimation of the modification coefficients by

omitting the zero- and first-degree terms of the modifier. In this scheme, the Stokes-integrated quasigeoid heights depend on two parameters: L (spherical harmonic degrees removed from the kernel) and ψ_0 (integration cap radius). These parameters were optimised through testing of the quasigeoid against GPS/levelling points (see Section 3 for the method and results).

The Stokes integrations were run on a very-high-performance supercomputer that is part of the iVEC Western Australian Supercomputer Program. A 192 CPU SGI Altix 3700 Bx2 computer with 366 GB of RAM and a 12 TB high-speed disk (http://www.ivec.org/) was used from this facility. This reduced the required computation time to ~6 hours from ~40 hours on a 2x 1.6GHz CPU Sun Ultra 45 workstation with 2 Gb of RAM per parameter combination.

L. Restoration of the reference field

The reference EGM2008 height anomaly grid (step I) is added to the residual quasigeoid heights from Stokes integration (step K), yielding each quasigeoid model. The magnitude and spatial distribution of the residual quasigeoid heights are shown in Fig. 11. Descriptive statistics are shown in Table 2. The residual quasigeoid heights presented here are based on kernel modification degree $L = 40$ and integration cap radius $\psi_0 = 2.5^\circ$. These were determined to be the optimal parameter combination (see Section 3).

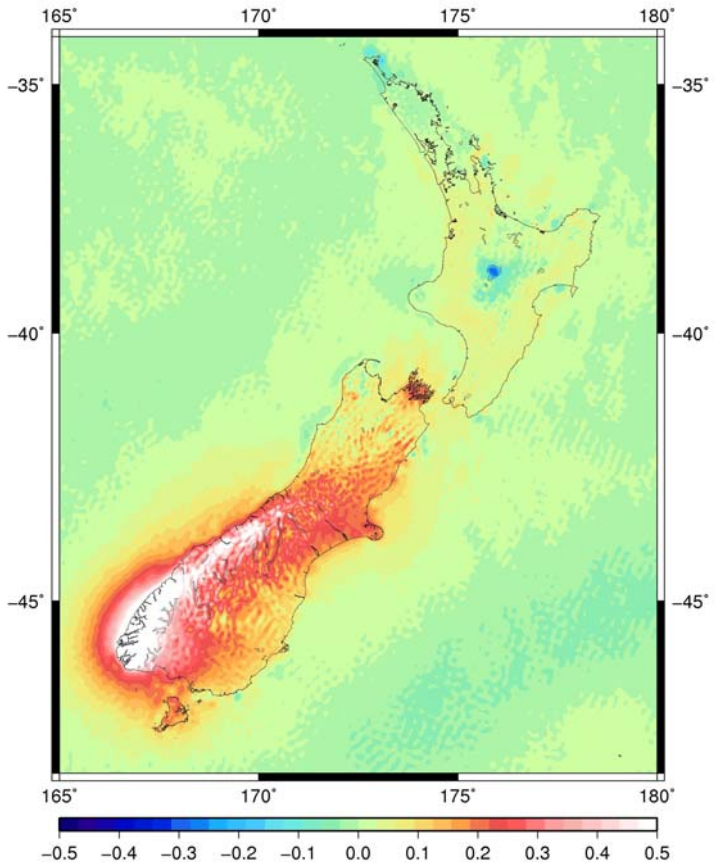

Fig. 11. Residual quasigeoid heights. (Mercator projection; units in m).

Table 2. Descriptive statistics of EGM2008 height anomalies and residual quasigeoid heights (units in m)

grid	min	max	mean	std.dev.	RMS
Reference quasigeoid	-46.679	54.277	5.979	28.251	28.877
Residual quasigeoid	-1.244	1.312	0.002	0.054	0.054

M. Geoid testing using GPS/levelling

In order to assess the computed quasigeoid heights, the 1422 "directly observed" quasigeoid heights from GPS/levelling are used for comparison (cf. Featherstone 2001). Figure 12 (left) shows the differences between the computed quasigeoid heights from step L, and quasigeoid heights from GPS/levelling, based on kernel modification degree $L = 40$ and integration cap radius $\psi_0 = 2.5^{\circ}$. Figure 12 reveals almost exclusively negative differences due to the deficient zero-degree term, as well as jumps of up to 0.2 m among neighbouring LVDs.

The differences between the GPS/levelling and quasigeoid are 'debiased' by subtracting the mean of the differences, computed for each LVD individually. These means are the LVD offsets used to compute the LVD correction to the gravity anomalies (step C), after which steps D to M are performed again until the LVD offsets converge (the iterative gravimetric quasigeoid computation process). The 'debiased' differences between NZGeoid09 and the 1422 GPS/levelling points are shown in Fig. 12 (right). A further analysis of the results for different parameter settings is provided in Section 3.

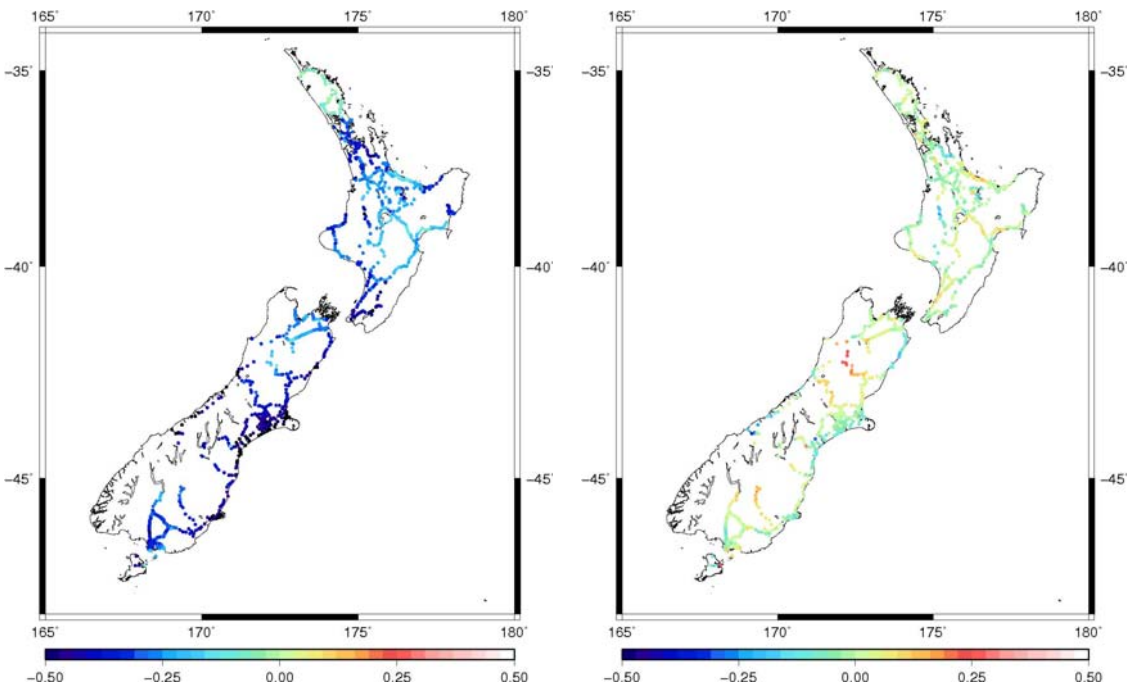

Fig. 12. Left: differences between NZGeoid09 and GPS/levelling; Right: debiased differences between NZGeoid09 and GPS/levelling (Mercator projections; units in m)

2.3 Summary of improvements

This section provides an overview of the improvements of NZGeoid09 over NZGeoid05 and its input data and computation strategy. For each improvement, the dataset or computation step is indicated between brackets.

Input data improvements

- Use of DNSC08 gravity anomalies on sea (dataset 3)
- Use of EGM2008 global gravity model (dataset 6)

Computational improvements

- Use of 1′x1′ grid resolution (NZGeoid05 computations were based on a 2′x2′ grid resolution) (steps E-M)
- Use of DNSC08 data as reinforcement for interpolation of land gravity data near the coastlines (step E)
- Use of improved version of *bin2sid* for the correct conversion of reconstituted Faye anomalies without truncation to integer mGal values (step F)
- Computation of rigorous area mean values of reconstituted Faye anomalies using sophisticated regridding techniques (*regrid_sid*; step G)
- Appropriate use of GMT masking operations for merging of land/sea anomalies with the high-resolution shoreline (step H)
- Computation of precise EGM2008 gravity anomaly area mean values in ellipsoidal approximation (step I)
- Computation of the residual quasigeoid using a slightly improved determination of the kernel modification parameters (step K)

3 Results and Analysis

The data processing scheme, as described in Section 2, was used for numerous computations of the New Zealand quasigeoid with different parameter settings. In Section 3.1, the results of the iterative computation of LVD offsets are shown. Section 3.2 shows the optimisation process of the quasigeoid computation using different Stokesian integration parameters. In Section 3.3, the optimised NZGeoid09 solution is compared to EGM2008 and GPS/levelling data, showing it to be an improvement.

3.1 Iterative computation of LVD offsets

Following the Amos and Featherstone (2009) approach, NZGeoid09 was obtained based on iterative computations of the vertical offsets *o*. Introducing 0.00 m as initial offsets for all LVDs, convergence was reached after just two iterations. It can be seen in Table 3 that the offsets computed differ considerably from the offsets computed in Amos and Featherstone (2009), especially on the North Island, even though offsets of LVDs on the North Island convergence faster than those on the South Island.

Table 3. LVD offsets after 2 iterations (based on L =40, ψ_0 = 2.5˚), as well as the offsets determined by Amos and Featherstone (2009), and the differences between the offsets of Amos and Featherstone (2009) and iteration 2 (units in m).

LVD	Iteration 2	A &F 2009	Difference
One Tree Point	-0.063	-0.242	0.179
Auckland	-0.339	-0.491	0.152
Moturiki	-0.241	-0.314	0.073
Gisborne	-0.344	-0.578	0.234
Taranaki	-0.315	-0.451	0.136
Napier	-0.203	-0.301	0.098
Wellington	-0.436	-0.504	0.068
Nelson	-0.294	-0.258	-0.036
Lyttelton	-0.466	-0.349	-0.117
Dunedin	-0.485	-0.485	0.000
Dunedin-Bluff	-0.381	-0.256	-0.125
Bluff	-0.360	-0.376	0.016
Stewart Island	-0.385	-0.400	0.015

Differences between the offsets of neighbouring LVDs are compared to the differences obtained from precise levelling (Table 4). It can be seen that the LVD offsets computed here agree better with the levelling observations than the offsets determined by Amos and Featherstone (2009) for all but three of the differences. Note, however, that some of these vertical datums (Dunedin-Bluff and Stewart Island are poorly realised vertical datums (Amos and Featherstone 2009).

Table 4. Comparison of differences between LVD offsets obtained after 2 iterations (based on $L = 40$, $\psi_0 = 2.5^\circ$) to offsets determined by Amos and Featherstone (2009; Table 2) and observed precise levelling offsets (units in m)

From	To	Iteration 2	A&F 2009	Levelling
Auckland	One Tree Point	-0.276	-0.249	-0.206
Auckland	Moturiki	-0.098	-0.177	-0.070
Gisborne	Moturiki	-0.103	-0.264	-0.075
Gisborne	Napier	-0.141	-0.277	-0.166
Moturiki	Napier	-0.038	-0.013	-0.099
Taranaki	Napier	-0.112	-0.150	-0.046
Taranaki	Wellington	0.121	0.053	0.147
Taranaki	Moturiki	-0.074	-0.137	-0.162
Napier	Wellington	0.233	0.203	0.237
Nelson	Lyttelton	0.172	0.091	-0.027
Lyttelton	Dunedin	0.019	0.136	-0.071
Dunedin-Bluff	Dunedin	0.104	0.229	-0.019
Dunedin-Bluff	Bluff	-0.021	0.120	-0.001

It should be noted that the offset values are sensitive to the choice of Stokes integration parameters that the quasigeoid computation is based on. This is seen by a comparison of the offsets obtained from an $L = 40$, $\psi_0 = 2^\circ$ quasigeoid with those obtained from parameters $L = 40$, $\psi_0 = 2.5^\circ$ and $L = 100$, $\psi_0 = 3^\circ$ (Table 5). Table 5 shows that the LVDs located on the mountainous South Island are particularly sensitive to parameter settings. This is because the residual gravity anomalies are larger in this region (Fig. 10), so the Stokesian contribution is correspondingly larger (Fig. 11).

For the sake of completeness, Table 5 also lists the offsets as obtained from an experimental quasigeoid solution using an EGM2008 reference field up to degree and order 360 only, as well as offsets from a the EGM2008 reference height anomalies only. This experiment was performed to verify that the computations were correct. The fact that the maximum degree of the EGM2008 reference field has little impact on the offsets indicates the Stokes integration yields results similar to the EGM2008 global gravity model, certainly in the spectral range from degree 361 to 2160.

Table 5. LVD offsets based on different Stokes integration parameters and different degrees of the EGM2008 reference field, and offsets obtained from EGM2008 only (units in m)

Model	**Quasigeoid**	**Quasigeoid (= NZGeoid09)**	**Quasigeoid**	**Quasigeoid**	**EGM2008 only**
Iterations	**2**	**2**	**2**	**2**	N/A
Stokes integration parameters	$L = 40$, $\psi_0 = 2^o$	$L = 40$, $\psi_0 = 2.5^o$	$L = 100$, $\psi_0 = 3^o$	$L = 40$, $\psi_0 = 2.5^o$	N/A
Degree of EGM08 reference grid	2160	2160	2160	360	2160
One Tree Point	-0.062	-0.063	-0.060	-0.064	-0.066
Auckland	-0.336	-0.339	-0.329	-0.338	-0.305
Moturiki	-0.236	-0.241	-0.230	-0.246	-0.219
Gisborne	-0.341	-0.344	-0.337	-0.354	-0.312
Taranaki	-0.310	-0.315	-0.303	-0.317	-0.285
Napier	-0.199	-0.203	-0.193	-0.208	-0.164
Wellington	-0.428	-0.436	-0.414	-0.440	-0.372
Nelson	-0.281	-0.294	-0.260	-0.307	-0.197
Lyttelton	-0.440	-0.466	-0.398	-0.473	-0.245
Dunedin	-0.452	-0.485	-0.419	-0.494	-0.334
Dunedin-Bluff	-0.336	-0.381	-0.267	-0.392	-0.120
Bluff	-0.320	-0.360	-0.266	-0.357	-0.174
Stewart Island	-0.351	-0.385	-0.307	-0.391	-0.166

Figure 13 shows the effect of the iterative computation strategy on NZGeoid09, using $L = 40$, $\psi_0 = 2.5^o$. This figure shows that systematic effects of up to 1.5 cm are mitigated by the Amos and Featherstone (2009) iterative approach, which would otherwise have been propagated directly into the NZGeoid09 solution.

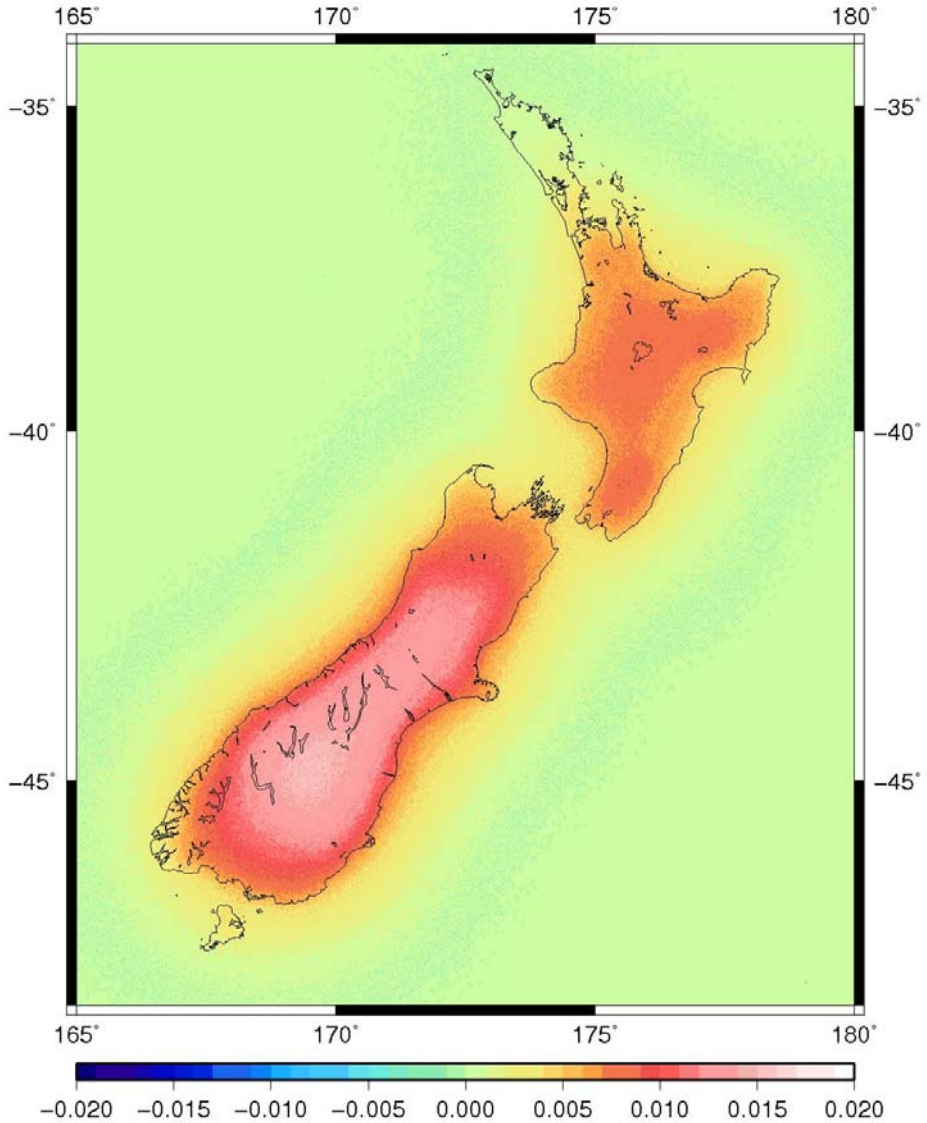

Fig. 13. Differences between NZGeoid09 and a quasigeoid without application of LVD corrections, both with Stokes integration parameters $L = 40$, $\psi_0 = 2.5^{\circ}$ (units in m)

3.2 Optimisation of the Stokesian integration parameters

A number of iterative quasigeoid computations have been performed according to the workflow described in Section 2, using a range of different Stokes integration parameters L and ψ_0. These computations are performed to find the optimum parameter combination, i.e., the quasigeoid which shows the smallest 'debiased' RMS error with respect to the GPS/levelling data.

The optimisation was performed in two steps. In the first step, all possible combinations of parameters $L = 40$, 180, 360 and $\psi_0 = 1^{\circ}$, 2°, 3°, 4°, 5°, 6° were used to compute quasigeoid grids. This first optimisation step covers a broad range of parameter choices and is aimed at roughly identifying which parameters yield an optimal solution. Then, in

a second optimisation step, more parameter choices in the vicinity of the optimum found in the first step are examined to find the optimal parameters with higher accuracy. Using this two-step approach, a large parameter space can be searched efficiently.

All computations are based on the Featherstone et al. (1998) modified Stokes kernel, as this is theoretically superior to and combines the best aspects of all previous deterministic modifications. The overall RMS values of the 'debiased' residuals resulting from the first optimisation step, obtained by comparison of the quasigeoids against the GPS/levelling data, are listed in Table 6. It can be seen that a modification degree $L = 40$ gives stable RMS values of 6.2-6.4 cm, whereas higher modification degrees yield larger RMS errors. This is because the kernel oscillates more for higher degrees, so its value at the centre of each cell in the numerical integration is not representative of the whole cell.

For the larger cap radii ψ_0 and $L = 40$, the RMS values do not vary much (Table 6). This indicates that there is not much problem with the propagation of low-frequency terrestrial gravity data errors into the solution (Vaníček and Featherstone 1998), which indicates that the iterative technique has effectively accounted for biases caused by the different LVDs. Table 6 indicates that the optimum is likely to be found in the vicinity of $L = 40$ and $\psi_0 = 2°$. Therefore, in the second optimisation step parameter choices close to these values are examined. All possible combinations of parameters $L = 20, 40, 60, 80, 100$ and $\psi_0 = 1.0°, 1.5°, 2.0°, 2.5°, 3.0°, 3.5°, 4.0°$ were used in this second step.

Table 7 shows the results of the second optimisation step, yielding almost identical RMS values of ~6.2-6.4 cm for each parameter combination. Hence, there is only a weak dependency of the RMS values on the Stokes parameters used when $L < 100$. A local minimum in the RMS errors (6.16 cm) is found for a cap radius ψ_0 of 2.5° and L between 20 and 60. For these parameter choices, a small change in the parameters has little influence on the resulting quasigeoid heights. **Based on these results, the new NZGeoid09 quasigeoid model is based on the parameters $L = 40$ and $\psi_0 = 2.5°$.**

Table 6. Optimisation step 1: RMS errors computed from differences between the GPS/levelling data and 18 different iterative quasigeoid computations with varying integration parameters L and ψ_0 (units in m)

$\psi_0 \downarrow$ L→	40	180	360
1°	0.064	0.064	0.065
2°	**0.062**	0.065	0.158
3°	0.062	0.066	0.092
4°	0.063	0.064	1.283
5°	0.063	0.113	0.101
6°	0.063	0.121	0.069

Table 7. Optimisation step 2: RMS errors computed from differences between the GPS/levelling data and 35 different iterative quasigeoid computations with varying integration parameters L and ψ_0 (units in m)

$\psi_0 \downarrow$ L→	20	40	60	80	100
1.0˚	0.0636	0.0636	0.0636	0.0637	0.0637
1.5˚	0.0621	0.0622	0.0622	0.0623	0.0624
2.0˚	0.0617	0.0617	0.0617	0.0618	0.0620
2.5˚	0.0616	**0.0616**	0.0616	0.0617	0.0619
3.0˚	0.0622	0.0620	0.0618	0.0617	0.0620
3.5˚	0.0629	0.0625	0.0620	0.0617	0.0624
4.0˚	0.0635	0.0629	0.0620	0.0615	0.0623

3.3 Final comparisons of NZGeoid09 to EGM2008 and GPS/levelling

Based on the analysis of parameter combinations in Section 3.2, NZGeoid09 is based on Stokes integration parameters $L = 40$ and $\psi_0 = 2.5^\circ$, and an EGM2008 reference field up to degree and order 2160. Figure 16 shows NZGeoid09 in the centre of the computation area and Fig. 17 shows the 'debiased' residuals with 1422 GPS/levelling points. The complete descriptive statistics (debiased) of the comparison of NZGeoid09 against GPS/levelling are found in Table 8. Additionally, height anomalies from EGM2008 only are also compared to the GPS/levelling dataset.

It can be seen from Table 8 that NZGeoid09 gives a slightly lower RMS error (6.2 cm) than EGM2008 (6.4 cm). Note that errors in the GPS and levelling observations also contribute to a lower bound on these differences. Table 8 also lists the descriptive statistics of the differences among NZGeoid09 and EGM2008 (which is identical to the sum of the residual quasigeoid heights), showing maximum differences of ~1.25 m in the Southern Alps.

Table 8 also shows the result of two experimental quasigeoid solutions with alternative parameter settings. The first (NZG360) is identical to NZGeoid09, except from the fact that the EGM2008 reference model is used up to degree and order 360 only (instead of 2160). This solution shows only small differences with NZGeoid09, indicating that the Stokes integration in the spectral range from degrees 361 to 2160 gives similar results to spherical harmonic synthesis of EGM2008 coefficients. The second experimental quasigeoid solution (NZG_unmodified) is based on Stokesian integration with an unmodified spherical kernel and a capsize of $\psi_0 = 179^\circ$, instead of the Featherstone et al. (1998) modified kernel. In this solution, the EGM2008 reference model is used up to degree and order 2160, as in NZGeoid09. The statistics of this solution show that it does not perform as well as NZGeoid09 and even worse than EGM2008, indicating that the modified kernel is better suited to the integration of residual gravity anomalies in New Zealand than the unmodified kernel. Both of these results affirm the applied computation strategy.

Figure 18 reveals that the maximum differences are found in Alpine areas of the South Island. The visible features represent the medium- and short-wavelength structures of the quasigeoid which are not delivered by the EGM2008 spherical harmonic series expansion

up to degree and order 2160. However, there is little coverage of the GPS/levelling observations in the mountainous regions of the South Island, so it is not so easy to gauge the improvements here. Figure 18 also shows relatively large negative differences between EGM2008 and NZGeoid09 around Lake Taupo in the central area of the North Island. The differences between NZGeoid09 and GPS/levelling shown in Fig. 17 indicate that NZGeoid09 performs significantly better in this area than EGM2008. Improvements in the GPS/levelling comparison are also seen in regions around Christchurch and Invercargill.

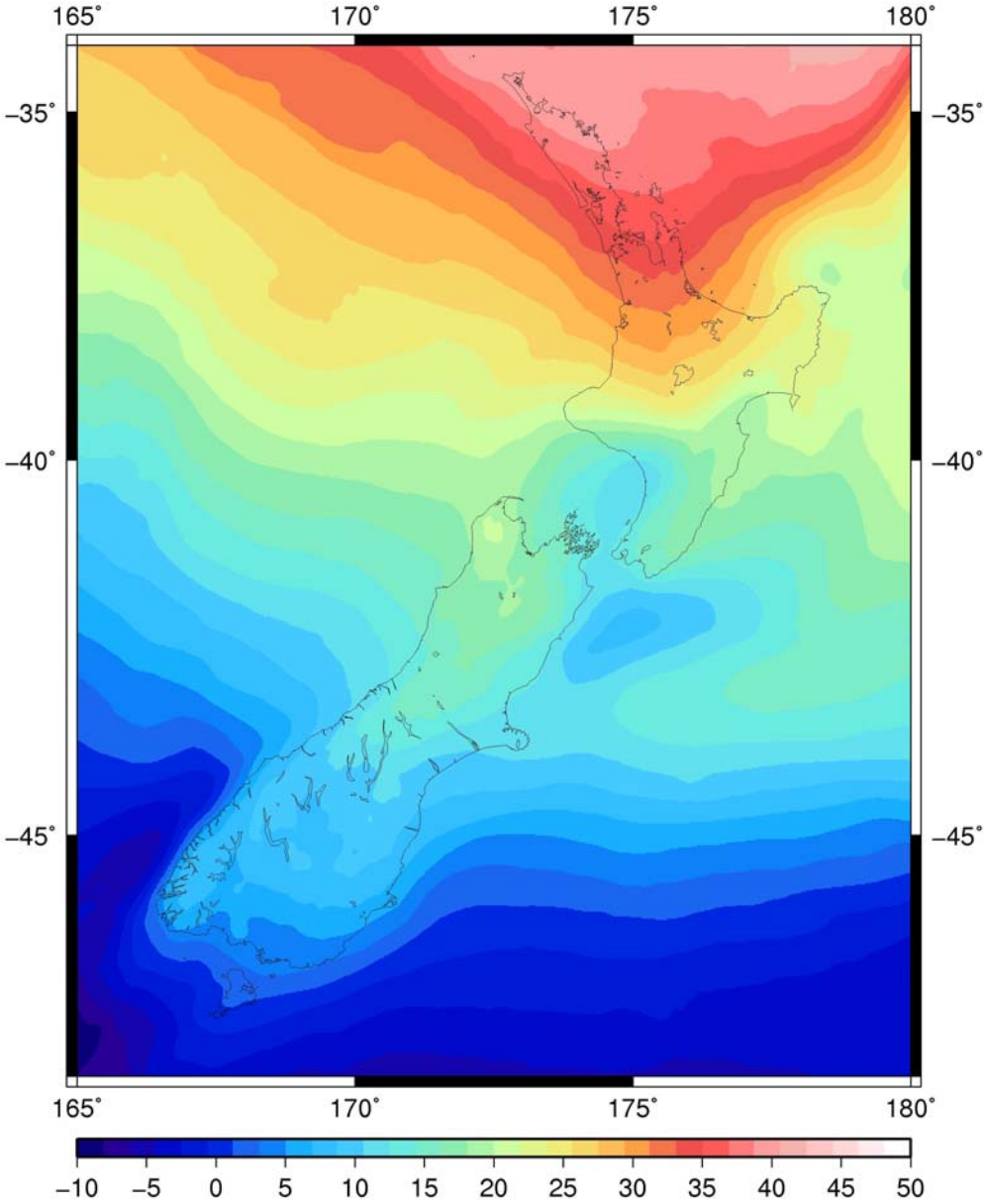

Fig. 16. NZGeoid09 quasigeoid heights in the central computation area (units in m)

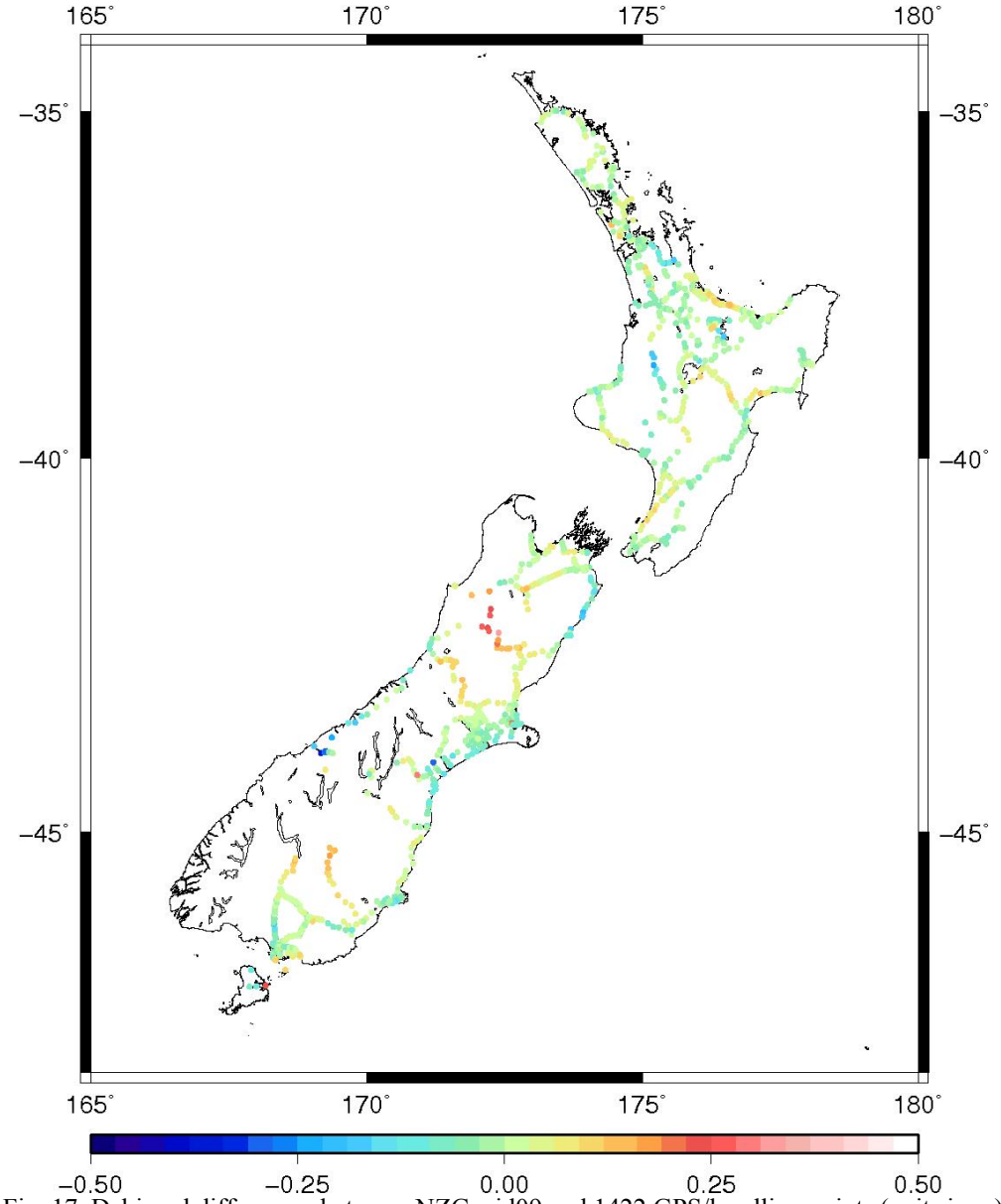

Fig. 17. Debiased differences between NZGeoid09 and 1422 GPS/levelling points (units in m)

Table 8. Descriptive statistics (debiased) of the comparisons of NZGeoid09, EGM2008, 1422 GPS-levelling observations, and two alternative quasigeoid solutions (units in m)

comparison	min	max	mean	RMS
NZGeoid09 – GPS/levelling	-0.378	0.280	0.000	0.062
EGM2008 – GPS/levelling	-0.284	0.337	0.000	0.064
NZGeoid09 – EGM2008	-1.244	1.259	0.001	0.051
NZG360– GPS/levelling	-0.369	0.348	0.000	0.063
NZG_unmodified– GPS/levelling	-0.426	0.304	0.000	0.066

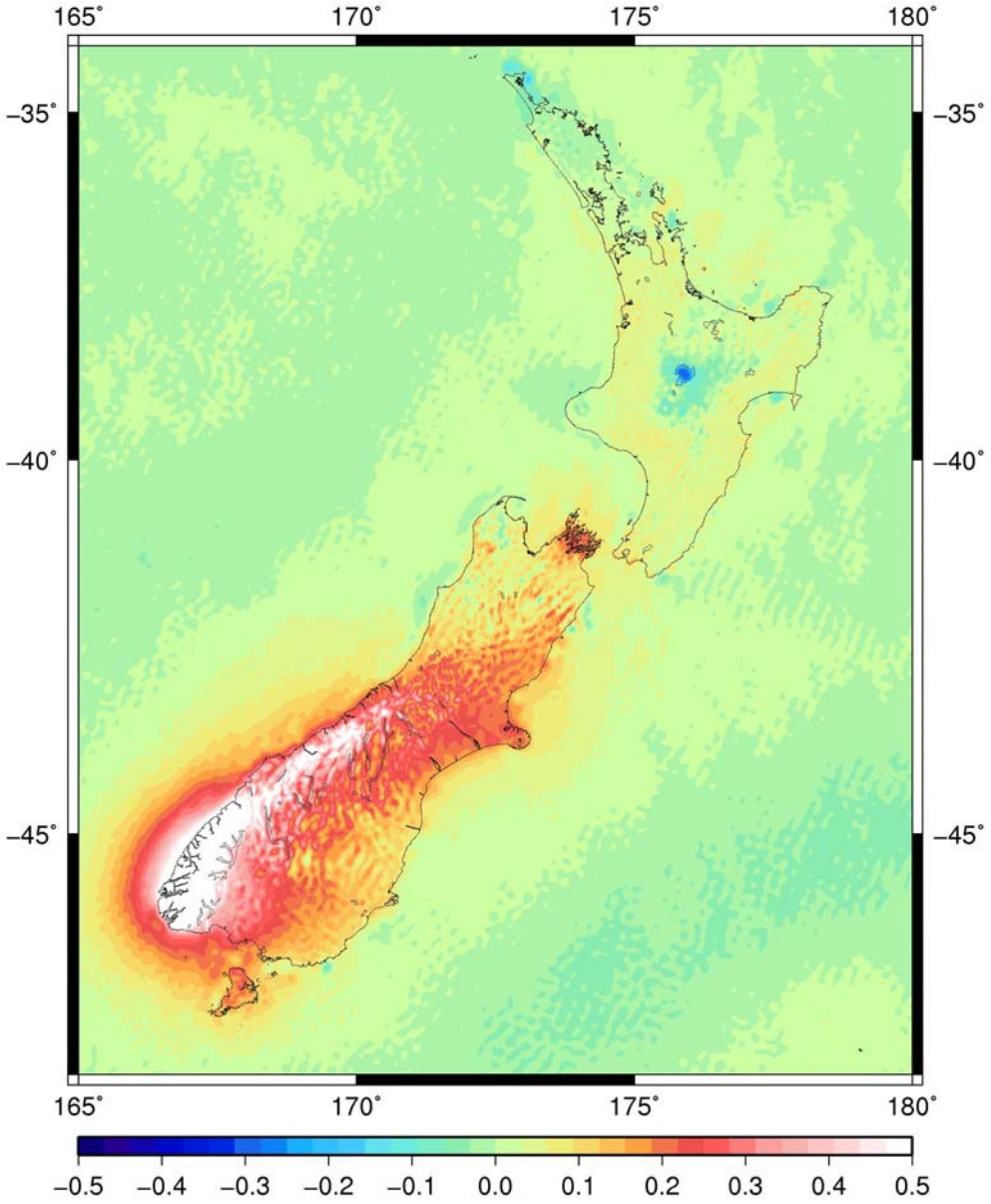

Fig. 18. Differences between NZGeoid09 and EGM2008 (units in m)

3.4 Final LVD offsets for NZGeoid09

The offsets of the LVDs as determined from the iterative computation of NZGeoid09 are summarised in Table 9. This information is also contained in Table 5, but is repeated here for ease of reference.

Table 9. LVD offsets for NZGeoid09 (units in m)

LVD	offset
One Tree Point	-0.063
Auckland	-0.339
Moturiki	-0.241
Gisborne	-0.344
Taranaki	-0.315
Napier	-0.203
Wellington	-0.436
Nelson	-0.294
Lyttelton	-0.466
Dunedin	-0.485
Dunedin-Bluff	-0.381
Bluff	-0.360
Stewart Island	-0.385

4 Concluding remarks

The new quasigeoid model for New Zealand, NZGeoid09, is a 1′x1′ gravimetric quasigeoid computed using the iterative gravimetric quasigeoid computation strategy of Amos and Featherstone (2009). The EGM2008 global gravity model is used up to degree and order 2160 as a reference model. Land gravity anomalies and marine gravity anomalies from the DNSC08 global model were used in the computation through Stokesian integration with the deterministic modified kernel of Featherstone et al. (1998).

Several improvements were made to the processing strategy used in the computation of NZGeoid05. Most notably, the interpolation of land gravity anomalies in coastal areas is reinforced through use of DNSC08 marine gravity anomalies, area means of reconstituted Faye anomalies are computed using a sophisticated regridding technique, and area means of gravity anomalies from EGM2008 are computed in ellipsoidal approximation. Some refined software packages were also used.

The optimal Stokes integration parameters of maximum degree of modification $L = 40$ and cap radius $\psi_0 = 2.5^\circ$ were determined through a comparison with 1422 GPS/levelling observations. The accuracy of the final NZGeoid09 is assessed using the same GPS/levelling dataset, yielding an overall standard deviation of 6.2 cm after removal of the vertical offsets from the residuals for each LVD. NZGeoid09 performs marginally better than the EGM2008 model, but additional GPS/levelling data in the Southern Alps are needed to confirm this further.

References

Amos, M.J. (2007) *Quasigeoid Modelling in New Zealand to Unify Multiple Local Vertical Datums*. PhD thesis, Curtin University of Technology, Perth, Australia.

Amos, M.J. and Featherstone, W.E. (2009) Unification of New Zealand's local vertical datums: iterative gravimetric quasigeoid computations, *Journal of Geodesy* 83(1): 57-68, doi: 10.1007/s00190-008-0232-y.

Anderson O.B., Knudsen, P., Berry, P. and Kenyon, S. (2008) The DNSC08 ocean wide altimetry derived gravity field. Paper presented at the 2008 General Assembly of the European Geosciences Union, Vienna, Austria, April 13-18, 2008.

Claessens, S.J. (2006) *Solutions to the ellipsoidal boundary value problems for gravity field modelling*. PhD thesis, Curtin University of Technology, Perth, Australia.

Claessens, S.J. and Anjasmara, I.M. (2008) EGM2008 Evaluation for New Zealand, consultancy project report to Land Information New Zealand, contract #CON-SE-DSS-TS-44657-1, Western Australian Centre for Geodesy, Curtin University of Technology, Perth, Australia.

Featherstone, W. E. (2001) Absolute and relative testing of gravimetric geoid models using Global Positioning System and orthometric height data, *Computers and Geosciences*, 27(7): 807-814, doi: 10.1016/S0098-3004(00)00169-2.

Featherstone, W.E. and Kirby, J.F. (2000) The reduction of aliasing in gravity anomalies and geoid heights using digital terrain data, *Geophysical Journal International*, 141(1): 204-212, doi:10.1046/j.1365-246X.2000.00082.x.

Featherstone, W.E., Evans, J.D. and Olliver, J.G. (1998) A Meissl-modified Vanicek and Kleusberg kernel to reduce the truncation error in gravimetric geoid computations, *Journal of Geodesy*, 72(3): 154-160, doi: 10.1007/s001900050157.

Forsberg, R. (1984) A study of terrain corrections, density anomalies and geophysical inversion methods in gravity field modelling. Report 355, Department of Geodetic Science and Surveying, Ohio State University, Columbus, USA.

Haagmans, R., de Min, E. and van Gelderen, M. (1992) Fast evaluation of convolution integrals on the sphere using 1D FFT, and a comparison with existing methods for Stokes' integral, *Manuscripta Geodaetica*, 18: 227-241.

Hipkin, R.G. (2004) Ellipsoidal geoid computation, *Journal of Geodesy*, 78(3): 167-179, doi: 10.1007/s00190-004-0389-y.

Hwang, C., Guo, J., Deng, X., Hsu, H.Y. and Liu, Y. (2006) Coastal gravity anomaly from retracked Geosat/GM altimetry: improvement, limitation and the role of airborne gravity data, *Journal of Geodesy*, 80(4): 204-216, doi: 10.1007/s00190-006-0052-x.

Pavlis, N.K., Holmes, S.A., Kenyon, S.C. and Factor, J.K. (2008) An Earth Gravitational Model to degree 2160: EGM2008. Paper presented at the 2008 General Assembly of the European Geosciences Union, Vienna, Austria, April 13-18, 2008.

Sideris, M.G. (1990) Rigorous gravimetric terrain modeling using Molodensky's operator, *Manuscripta Geodaetica*, 15: 97-106.

Smith, W. H. F. and Wessel, P. (1990) Gridding with continous curvature splines in tension, *Geophysics*, 55 (3): 293-305.

Torge, W. (2001) *Geodesy*. Second Edition. W. de Gruyter, Berlin, New York.

Wessel, P. and Smith, W. H. F. (1998) New, Improved Version of Generic Mapping Tools Released, *EOS Transactions, American Geophysical Union*, 79(47): 579.

Appendices

A1. Overview of software and jobfiles used in the computation of NZGeoid09

Table 10 contains an overview of the main jobfiles and the scripts and software these call, while Table 11 gives an overview of jobfiles called in the main jobfiles. The tables also refer to the computation steps (A-M) the job files perform. A description of these steps is provided in Section 2 and Fig. 2. All jobfiles are well-documented to help understand the data flow.

Table 10. Main jobfiles

Jobfile	**Steps**	**Uses (scripts, software)**
geoidmain_part1.job	A,B	
	A	nz_extract_boug.job
	B	nz_refine_boug.job
nz_ggm.job	I	harmonic_synth_nz_inp_am, harmonic_synth_nz_inp_sp, grdmath
geoidmain_part2.job	C,E,F, G,H,J, (K)	
	C	awk
	E	surface
	F	ni_reconst1.job, si_reconst1.job
	G	faye_regrid.job
	H	grdlandmask, grdmath
	J	sidmath
	K	FFT1Dmod2009 (use of supercomputer iVEC)
geoidmain_part3.job	L, M	
	L	sidmath
	M	gps_lev_testing.job

Table 11. Jobfiles called by main jobfiles

Jobfile	**Steps**	**Uses (scripts, software)**
nz_extract_boug.job	A	nzanom_extract , nzgrav_anom_datum
nz_refine_boug.job	B	tc_applicator
ni_reconst1.job	F	ni_reconstitute_1min, sid2bin, bin2sid
si_reconst1.job	F	si_reconstitute_1min, sid2bin, bin2sid
faye_regrid.job	G	regrid_sid
gps_lev_testing.job	M	geoid_fit_debias, geoid_fit_dumper

A2. Overview of directory structures

Table 12 shows the directory structure of the input data for NZGeoid09 (data/). Table 13 shows the structure of the results directory (results/). The directory structure is set up to provide easy access to all input and output files generated for the NZGeoid09 computation. The directory names directly refer to the steps in the computation process shown in Fig. 2. Besides the data (grid-files, statistics-files), each of the directories contains figures in eps and jpg format, which help to better understand and interpret the results. The results provided refer to the optimum Stokes integration parameters (L = 40 and ψ_0 = 2.5˚).

Table 12. Input data directory structure

No	Directory name	Description/content	Step accessing the data
1	gravanom/	13 files containing the NZ gravity data base, separately for each LVD (+1 file for Chatham Islands)	A
2	prismtc/	62 tiles of 1′ x 1′ NZ precomputed terrain corrections (resolution: 1.8″)	B
3,4	DNSC08/	DNSC08 altimetry only and DNSC08 draped (altimetry + shiptrack data); 1′ free-air anomalies	H
5	dem/	62 tiles of 1′ x 1′ NZ national elevation data (resolution 1.8″)	F
6	ggm/	EGM2008_to2190_TideFree spherical harmonic coefficient file	I
7	gpslev/	13 files containing the NZ GPS/levelling data, separately for each LVD (+1 file for complete NZ)	M

Table 13. Results directory structure

Directory name	Description/content
A_scatboug	Scattered Bouguer anomalies (for all LVDs)
B_refboug	Refined Bouguer anomalies (for all LVDs)
C_LVDcorrboug	LVD-offset corrected refined Bouguer anomalies (for all LVDs)
D_suppmarinegrid	DNSC08 1′ marine grid (masked, to be used as supplement for the land Bouguer interpolation)
E_griddedboug	1′ gridded land Bouguer anomalies
F_griddedfaye	1.8″ gridded land Faye anomalies
G_blockedfaye	1′ area mean land Faye anomalies
H_mergedanomalies	Merged land/sea anomalies (land anomalies from step G and DNSC08 sea anomalies from /data/)
I_ggmgrids	EGM2008 height anomaly and gravity anomaly reference grids
J_resgravity	Residual gravity anomalies
K_resgeoid_from_IVEC	Residual quasigeoid heights from Stokes integration (results from *FFT1Dmod2009* on supercomputer iVEC)
K_resgeoid	Statistics and figures of residual quasigeoid heights
L_nzgeoid09	NZGeoid09 (obtained from EGM2008 restoration)
M_gpstesting	Residuals and debiased residuals of NZGeoid09 with respect to the GPS/levelling data

A3. Visualisation of the NZGeoid09 computation process for a 1˚ x 1˚ test tile

In this appendix, the complete quasigeoid computation process is visualised for a selected 1˚x1˚ tile (Northern Fiordland, South Island, 168˚E/169˚E/45˚S/44˚S). The set of maps in Fig. 19 shows the spatial resolution and the magnitudes of the gravity anomalies, quasigeoid heights and terrain heights that occur at different stages of the quasigeoid computation. The letters introducing the captions refer directly to the computation steps in Fig. 2.

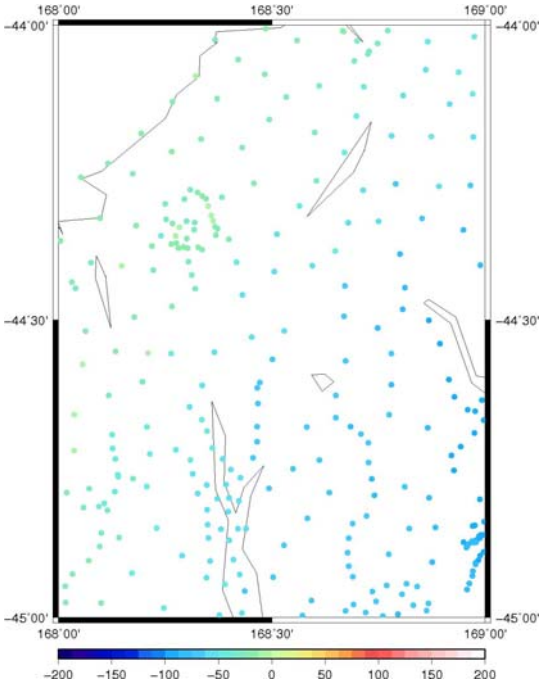

A output: Bouguer anomalies extracted from the NZ database at scattered locations (units in mGal)

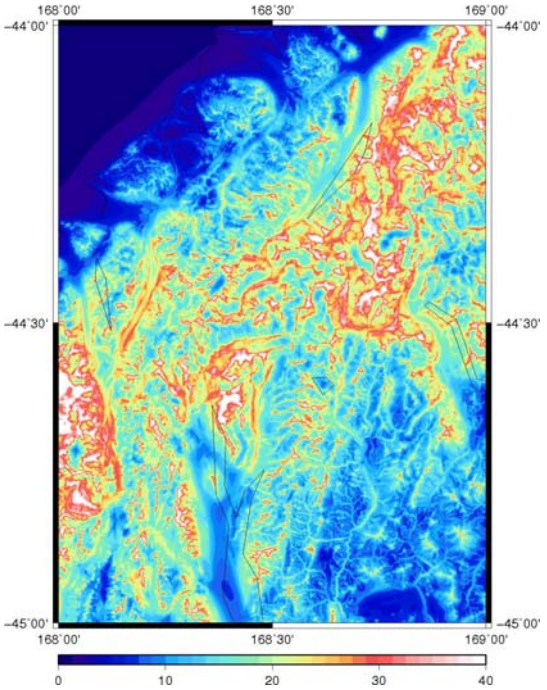

B input: Grid of terrain corrections used to refine the Bouguer anomalies from A (units in mGal)

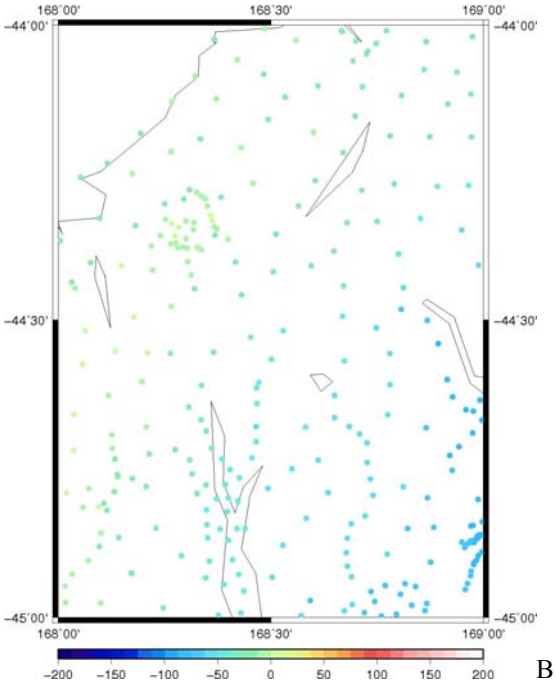

B output: refined Bouguer anomalies at scattered locations (units in mGal)

B

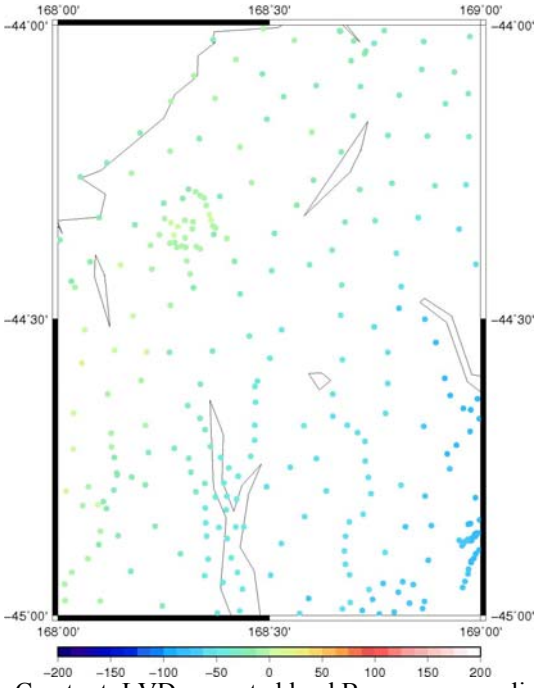

C output: LVD corrected land Bouguer anomalies (units in mGal)

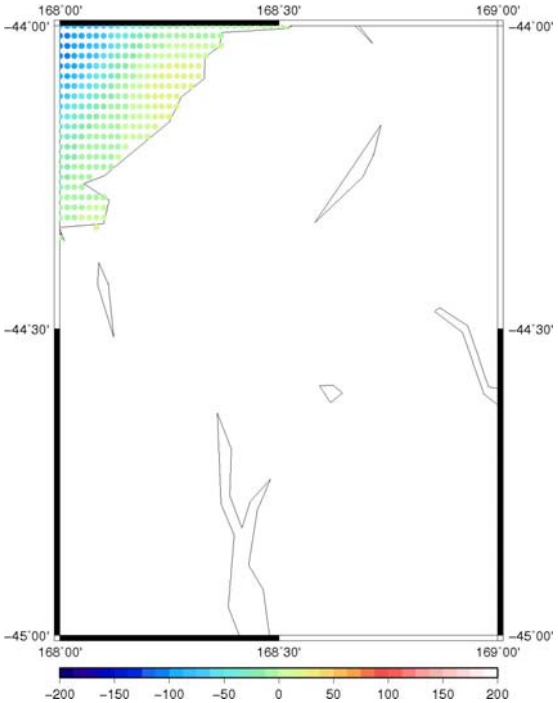

D output: masked DNSC08 marine free-air anomalies (to be used as reinforcement for step E) (units in mGal)

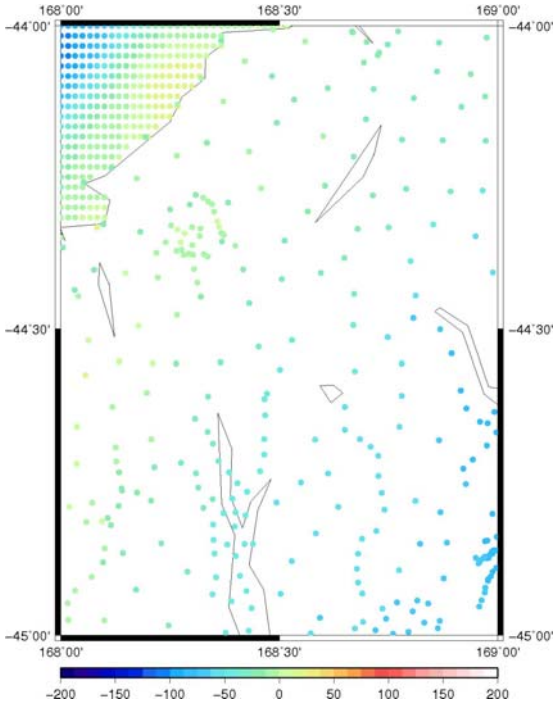

E input: merged datasets C and D (units in mGal)

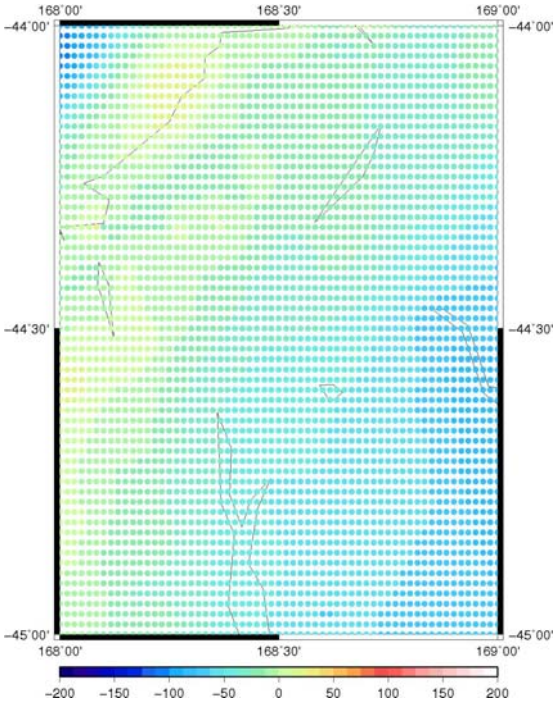

E output: 1′ gridded Bouguer anomalies (units in mGal)

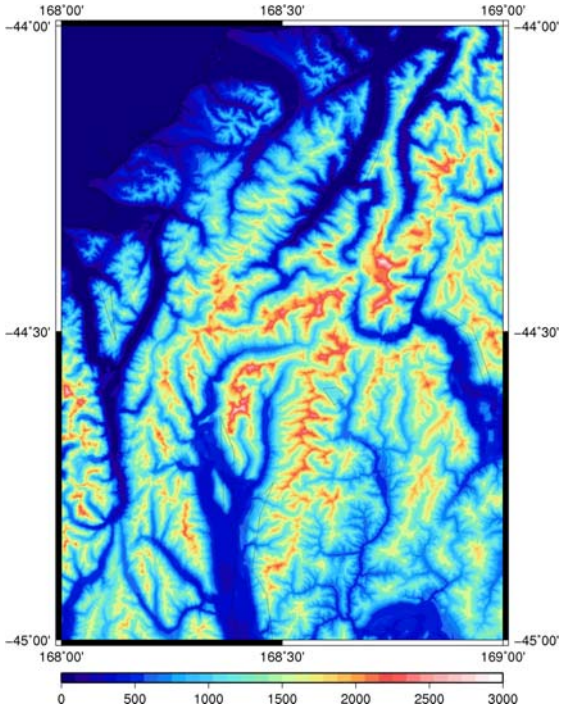

F input: DEM Data at 1.8″ resolution (units in m)

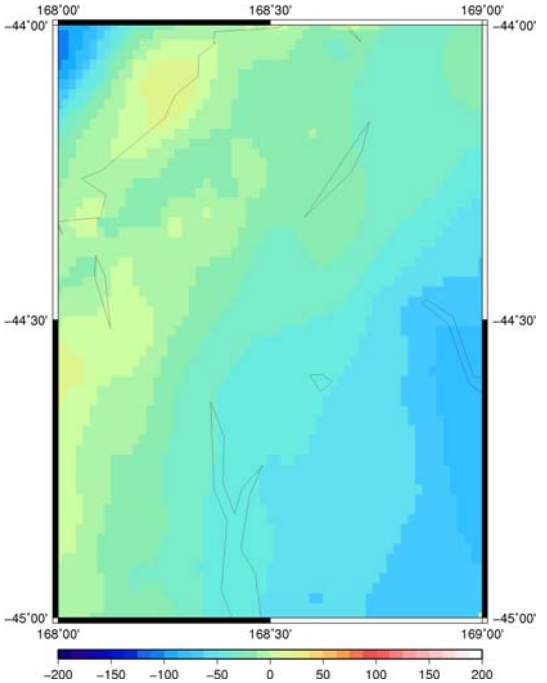

F input: 1´ gridded Bouguer anomalies (identical to E output; units in mGal)

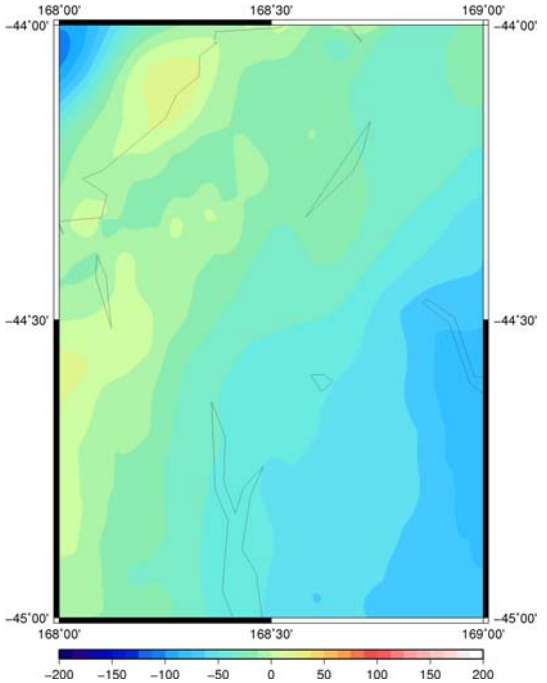

F intermediate result: 1.8″ interpolated Bouguer anomaly grid (units in mGal)

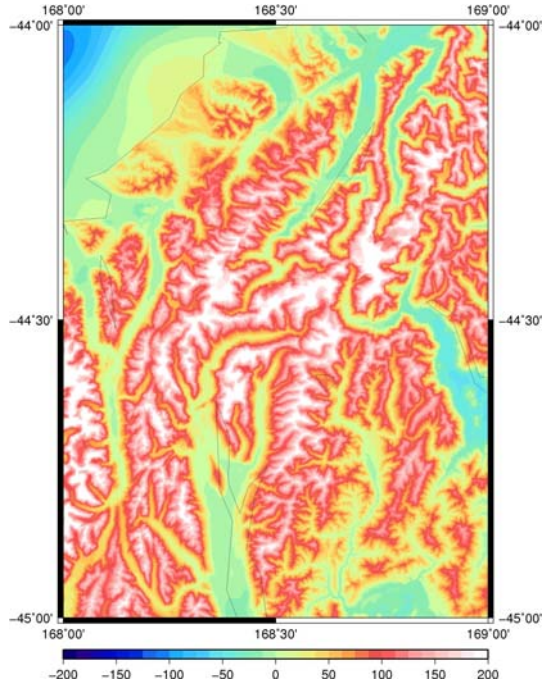

F intermediate result: 1.8″ grid of Bouguer plate corrections (units in mGal)

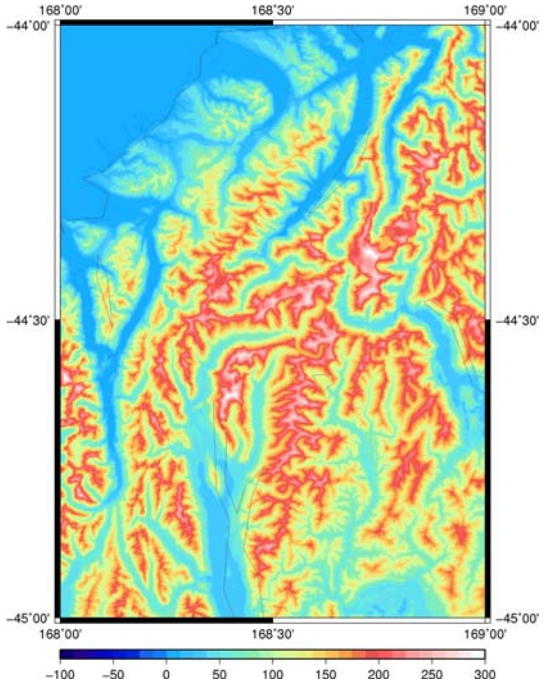

F output: 1.8” grid of Faye anomalies (units in mGal)

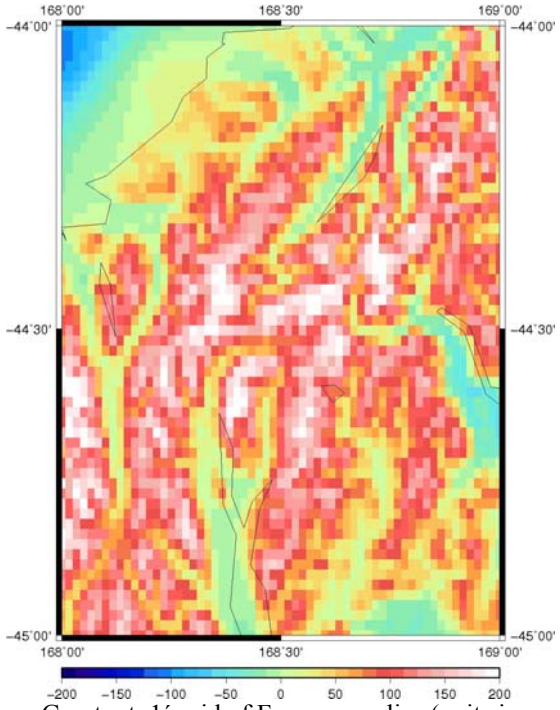

G output: 1′ grid of Faye anomalies (units in mGal)

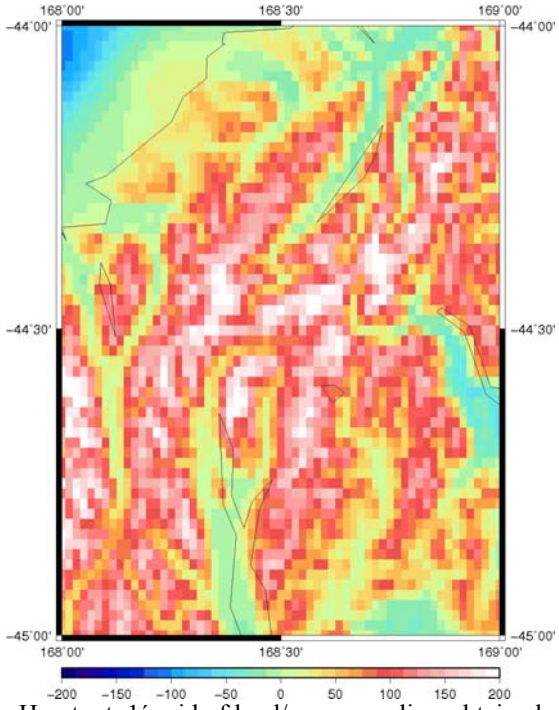

H output: 1′ grid of land/sea anomalies, obtained from merging DNSC08 with masked land Faye anomalies from G (units in mGal)

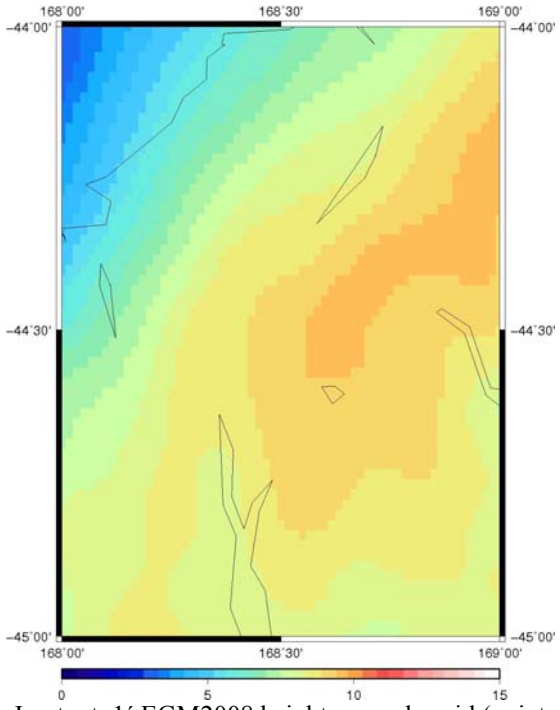

I output: 1′ EGM2008 height anomaly grid (point values), degrees 2-2160 (units in m)

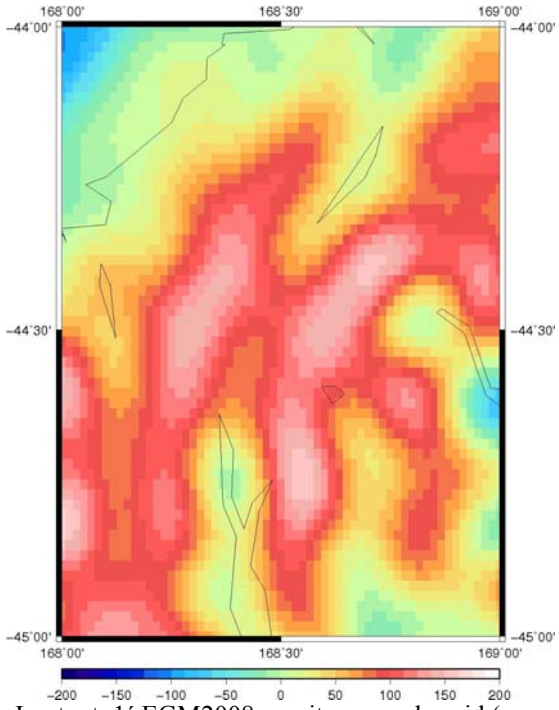

I output: 1′ EGM2008 gravity anomaly grid (area means in ellipsoidal approximation), degrees 2-2160 (units in mGal)

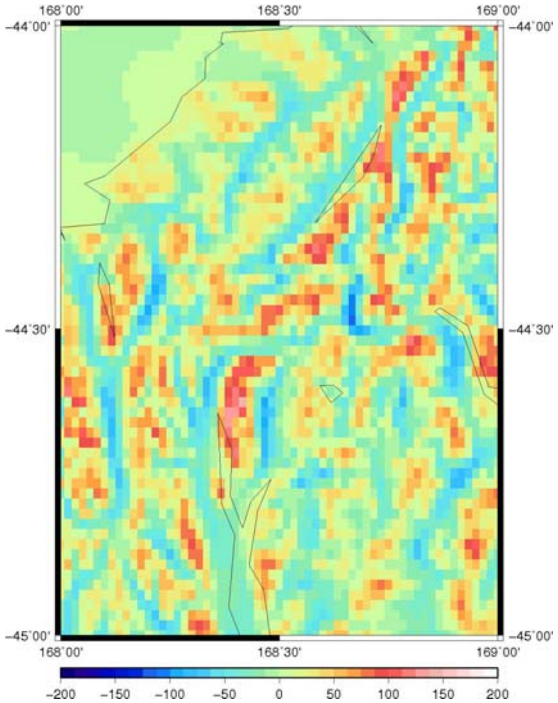

J output: 1′ residual gravity anomaly grid (units in mGal)

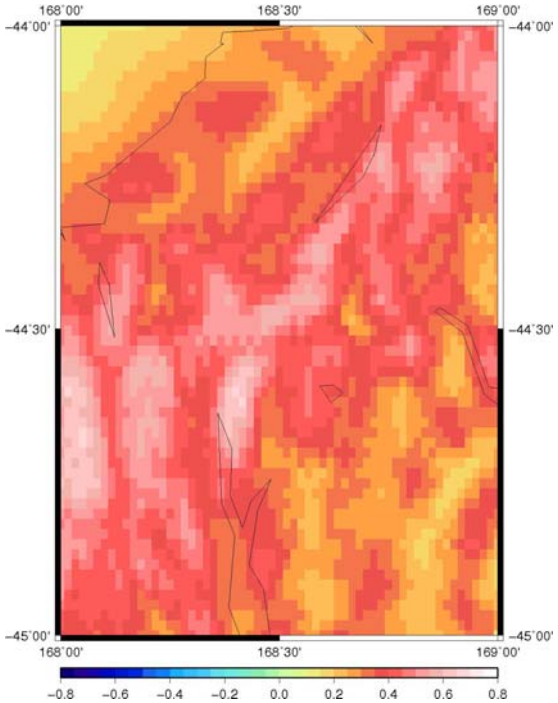

K output: 1′ residual height anomaly grid from Stokes integration (units in m)

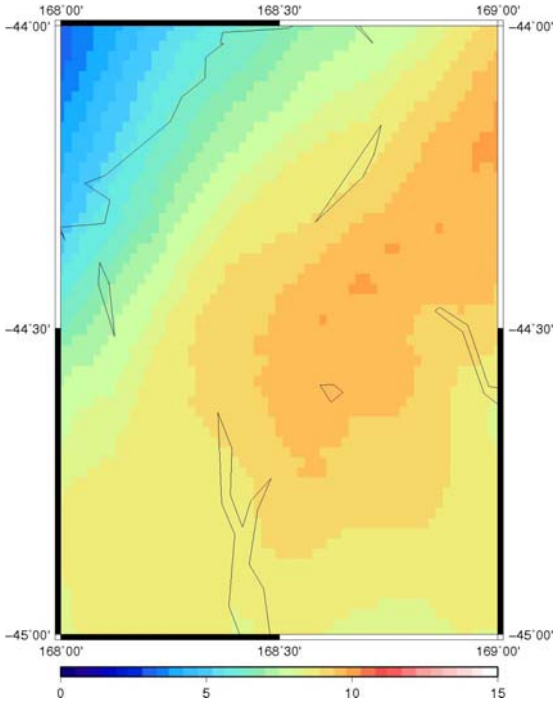

L output: 1′ quasigeoid height grid (units in m)

Figure 19. Overview of computation steps A-L for a 1˚x1˚ tile in Northern Fiordland, South Island (Mercator projections)